NTNU
Norwegian University of
Science and Technology

Multiscale modelling of fiber composites

Investigating micromechanics of
constituents' interaction

Sondre Østli Rokvam

Master of Science in Mechanical Engineering
Submission date: June 2018
Supervisor: Nils Petter Vedvik, MTP

Norwegian University of Science and Technology
Department of Mechanical and Industrial Engineering

Abstract

The objectives of this thesis have been to develop a script for a multiscale method based on first order homogenisation, to investigate estimation of properties and behaviour of unidirectional (UD) fiber composites.

To model composites on the microscale, an algorithm that generates periodic representative volume elements (RVE) geometries from controllable parameters and a pseudo random factor was developed. The output of this algorithm (fiber populations) was used to create heuristic RVE models in the Finite Element Analysis (FEA) software, Abaqus 6.14-4. These heuristic RVE models consist of fibers, matrix and an interface. The fibers in the models were assigned linear elastic material properties and the matrix and interface were assigned elastic, plastic and damage material properties.

To simulate deformations and loads, macro strains were imposed on the heuristic RVE models through constraint equations. As the properties of the RVE varied with the distribution of the fiber populations, the creation of RVE models was automated to perform multiple iterations to calculate estimations of the average properties and the statistical dispersion of these.

The effect of design parameters on stiffness estimations was investigated. To get insight into the local stress field in the RVE models, the maximum principal stress and maximum shear stresses were found for normalized linear elastic load cases. The strength of the RVEs was predicted by simulating nonlinear behaviour with different assigned material models. Consistent macrostrains for the non-linear analyses were maintained by an iterative backward force balancing procedure.

The results showed that the stiffness estimations generally follow micromechanical approximations based on the rule of mixture. For the strength estimations, the produced results correlate with comparable methods and results found in the literature. This suggests that the method is feasible for microscale modelling of an RVE of UD fiber composites. Further development into material models, damage models and confirmation and calibration of results with empirical data should be investigated before using such a tool for design estimates.

Sammendrag

Målet med denne undersøkelsen var å utvikle et skript for en multiscale metode, basert på første ordens homogenisering, for å estimere egenskaper og oppførsel av pakkede ensrettet (UD) fiberkompositter.

For å modellere kompositter på mikroskala ble en algoritme utviklet. Den genererer periodiske representative volumelementgeometrier (RVE-geometrier) fra kontrollerte parametere samt en pseudo-random faktor. Resultatene fra denne algoritmen (fiberpopulasjoner) ble brukt til å skape RVE-modeller i element metode programvaren, Abaqus 6.14-4. RVE-modellene består av fibre, matrise og grensesnitt. Fibrene i modellen ble tildelt lineær elastiske materialegenskaper. Matrisen og grensesnittet ble tildelt elastisk og plastiske materialegenskaper og enkle skade modeller.

For å simulere deformasjoner og belastninger ble RVE-modellene utsatt for makrotøyninger gjennom randbetingelser. Egenskapene til de representative volumelementene varierte mellom de forskjellige fiberpopulasjonene. For å undersøke effekten av forskjellige fiber populasjoner i RVE-modellene, ble scriptet automatisert for å kunne utføre flere iterasjoner av forskjellige RVE modeller for å beregne gjennomsnittlige estimater med statistisk avvik.

Effekten av designparametere på stivhetsestimater ble undersøkt. For å undersøke den lineære spenningsfordelingen i RVE-modellene ble maksimale hoved- og skjærspenninger for normaliserte elastiske belastningssaker beregnet. Styrken til RVEer ble testet ved simulering av ikke-lineær oppførsel. For å opprettholde den originale belastningstilstanden ble det undersøkt en bakoverseende iterasjonsmetode for justering av makrotøyningene.

Resultatene fra stivhetsestimatene samsvarer med mikromekaniske beregningsmodeller og styrkeresultatene samsvarer med resultater fra tidligere forskning. Metoden kan dermed antas å kunne brukes for modellering av kompositt egenskaper på mikroskala, men resultatene må bekreftes og kalibreres med empiriske data. Før det utviklede verktøyet kan brukes i produktutviklingssammenheng burde også materialmodeller og skademodeller utvikles videre.

Preface

This thesis is the final delivery in the study program Mechanical Engineering, Master of Science in Materials Science and Engineering at the Norwegian University of Technology and Science (NTNU). The project was carried out during spring 2018, as a continuation of a specialization project in the fall 2017. The learning curve has been steep due to little previous experience with the used software's and programming language.

I would like to thank my supervisor, Nils Petter Vedvik for the guidance, challenges and discussions, Abedin Gagani for sharing insight to composite and the modelling of these, and the composite group at the department for direction, discussions and given me possibility for further development.

I would also like to thank my family and my girlfriend for support through the studies.

Table of Content

List of Figures

List of Equations

Abbreviations

RVE - Representative Volume Element

RVE is the minimum cross section of a material on the microscale, which can be modelled to make accurate predictions of the macro. In this report, RVE refers to the RVEs of fiber composites.

SERVE – Statistically representative RVE

SERVE is an RVE which follows statistical distribution functions, like neighbour fiber distance or radial distributions, to increase the probability of an RVE geometry being realistic.

FEA/FEM - Finite Element Analysis/Method

FEM is a coarse graining modelling method, which simplifies a model by dividing the geometry of a structure into small elements interacting with each other.

UD – Unidirectional

When referring to a UD fiber configuration in a composite the fibers are parallel to each other.

1. Introduction

In this chapter are aspects of fiber composites, multiscale modelling and micro modelling introduced. After that are the objectives and the structure for this thesis presented.

1.1. Overview

In design cases where optimization between weight and strength is of importance, fiber composites have increasingly been applied due to their outstanding mechanical properties in combination with weight savings (Llorca et al., 2011). The increased use of composites has created a demand in the industries for better mechanical properties and improved understanding of characteristics like stiffness, strength and damage (Petersen, 2017). The estimation of these properties is vital to successfully design against damage and failure for longevity.

The damage progression in composites is a complex process with several failure mechanisms acting on different length scales. Due to this, data from experiments are traditionally used in estimation of properties in composite designs (Llorca et al., 2011). As experiments often are expensive and time-consuming, the use of computational modelling software is a cost-effective alternative. Since first introduced, computational modelling methods have proven their potential in discovering and designing materials with improved properties (Llorca et al., 2011).

Incremental advances in computational power, algorithms and engineering design tools are steadily making virtual testing more relevant. Although higher computational power gradually becomes more available, the current power is not sufficient for creating models that examine every aspect of realistic structures within a reasonable timeframe. Simplified models are therefore required to be able to make practical estimates. Pulungan, Lubineau, Yudhanto, Yaldiz, and Schijve (2017, p. 1) state that: *"to obtain the optimum design of composite materials with superior performance, manufacturing industries need to have a robust numerical tool to very quickly virtually test the influence of microstructural design parameters with respect to the damage behaviour of composites."* When modelling the effects of damage, it is often with respect to strength and stiffness to design against failure.

Like damage progression, mechanical properties like stiffness, strength and toughness depend on multiple processes which take place on various scales, from the nanoscale to meters.

Multiscale methods that model composite behaviour on different length scales are used together to predict behaviour for the whole structure. Multiscale methods on composite are illustrated in Figure 1.1. Such methods (Geers, Kouznetsova, & Brekelmans, 2010, p.1) *"…has contributed to considerable progress in bridging the field of mechanics of materials to the field of materials science."*

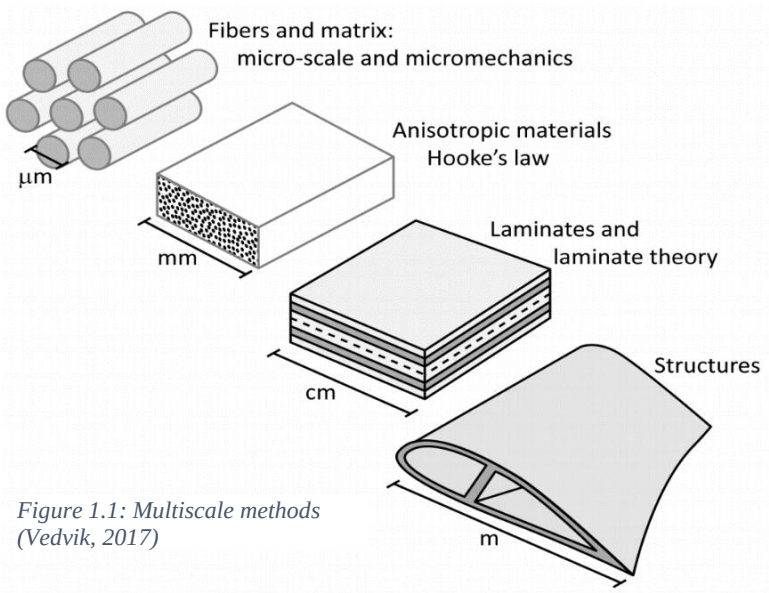

Figure 1.1: Multiscale methods (Vedvik, 2017)

The combination of existing material models with the computational power was envisioned around the 1960-70s. Pulungan et al. (2017, p.1) tell that: "*several researchers have successfully developed micromechanical models for fiber-reinforced composites to study phenomena like the effect of thermal residual stress on the damage initiation and prediction of damage evolution in woven composites*". Some of these micromechanical models have been applied with advanced material models to mimic behaviour like tensile and compression hardening and failure modes like cracking in the matrix and delamination of the interface (Naya, González, Lopes, Van der Veen, & Pons, 2017).

1.2. Multiscale modelling of fiber composites

By combining material properties based on data from the smaller length scales with the geometry from each investigated length scale, the total response of the design can be estimated. The strategy is illustrated in Figure 1.2.

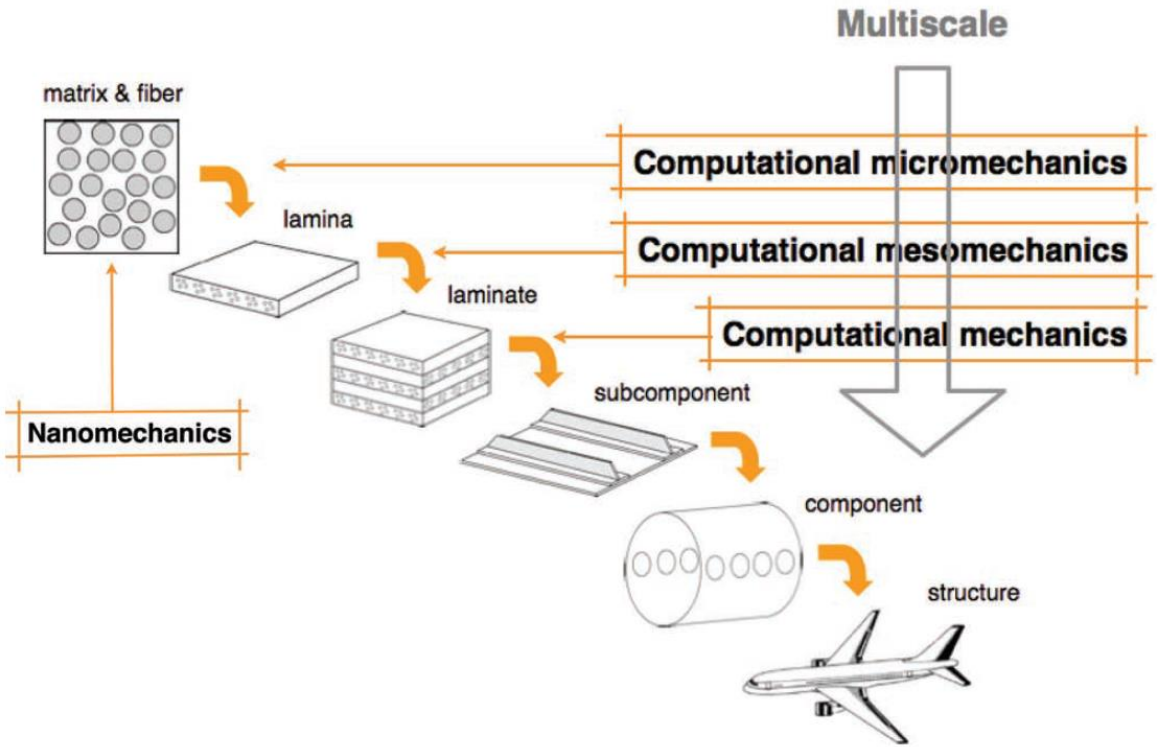

Figure 1.2: Modelling strategy (Llorca et al., 2011)

Since the component and laminate scale of composites are highly dependent on each individual design case, a bottom-up approach from computational micromechanics is commonly used in the application of the multiscale method (Llorca et al., 2011). While mechanical failure starts on the nanoscale, which is usually thought of as the lowest scale length of interest, this scale is highly influenced by chemistry (Petersen, 2017) and is therefore outside the scope of this thesis.

Due to the versatility of fiber composites, they are applied in a wide range of designs and will likely be exposed to a variety of multidirectional displacements and loads, depending on the design case. To get estimates of global stiffness and strength of the design, the properties are calculated from the behaviour at the microscale. By investigating composites behaviour when exposed to different stresses and strains at different length scales, a failure criterion for composites internal structures on the different length scales can be derived. These failure

criteria can be used to ensure that the composite's internal structures are dimensioned against abrupt failure.

1.3. Modelling composites on the micro scale

A modelling approach based on the concept of first order homogeneity with periodic boundary conditions is investigated in this thesis. When applied in a multiscale method the homogeneity assumes the principle of separation of scales. This implies that microscopic length scale is assumed to be much smaller than the macroscopic length scale (Geers et al., 2010). As illustrated in Figure 1.3, a material heterogeneous on the microscopic scale can be considered as homogenous on macroscopic scale. Estimations of properties like a homogenous anisotropic material (Figure 1.1) are based on constituent material properties and geometrical configuration on the microscale.

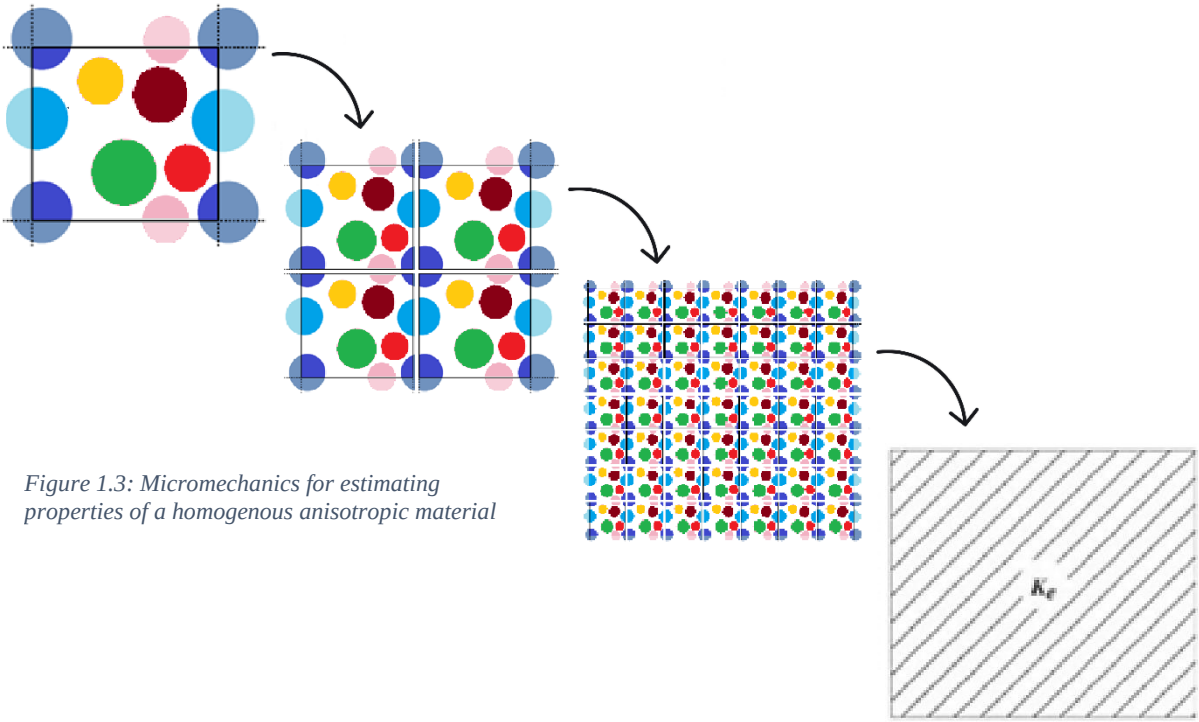

Figure 1.3: Micromechanics for estimating properties of a homogenous anisotropic material

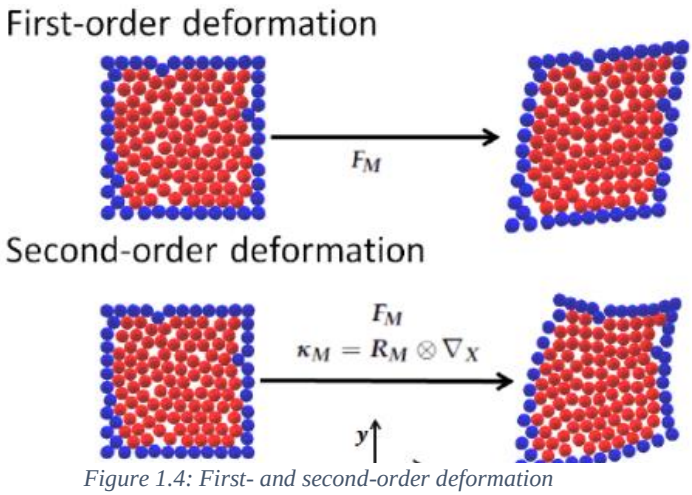

Figure 1.4: First- and second-order deformation (Wang & Sun, 2016)

By applying first order deformation, a continuous repeating periodic behaviour on the microscale can be assumed. The difference between first and second order deformation is that first order is composed of extension/compression and shear modes. In second-order deformation there are additional curvatures in the deformation (Figure 1.4).

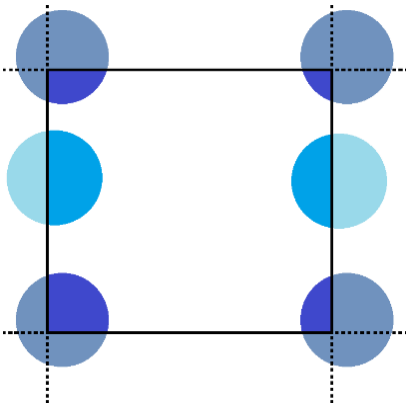

Figure 1.5: RVE with periodic boundary conditions.

To estimate material behaviour and properties of the fiber matrix structure on the microscale, the concept of the Representative Volume Element (RVE) or unit cell is introduced. RVEs are a microstructural sub-region which on average represents the entire microstructure (Swaminathan, Ghosh, & Pagano, 2005).

RVEs with periodic boundary conditions have proven to be most versatile for both periodic and non-periodic microstructures (Geers et al., 2010). To model periodic fiber composites fibers with parts outside the RVE border are continued on the other side of the RVE, as illustrated in Figure 1.5.

As the properties of a single RVE may vary for different distributions of fibers, an approach where several random generated RVEs, as illustrated in Figure 1.6, is investigated to get estimates and a statistical distribution.

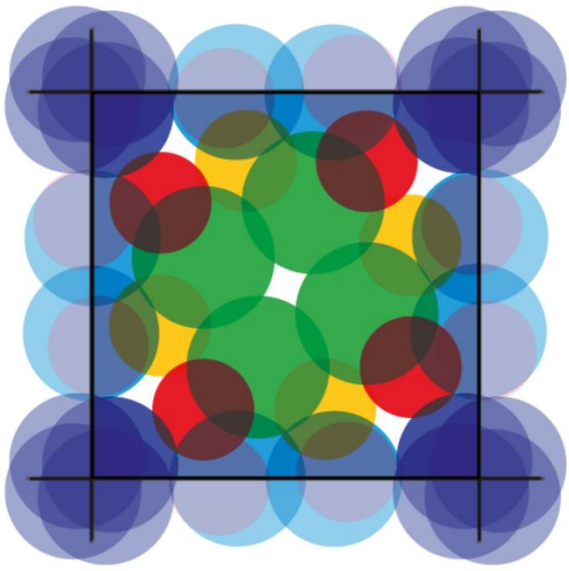

Figure 1.6: By generating several models the average properties can be estimated.

1.4. Objectives and limitations

The aim of this project is to develop and implement a framework for microscale modelling of unidirectional fiber composites. This is done by utilizing RVEs and finite element analysis (FEA) to identify macroscopic behaviour, like elastic properties, failure and damage evolution in the composite materials.

To assess how this method manages to capture composite behaviour and whether the results from simulations might provide any practical insight into composite performance, a virtual tool will be developed. This tool shall automate the generation of RVEs models in a FEA environment and simulate load and deformation cases designed for estimating stiffness and strength properties.

The project was defined as a feasibility study of a multiscale finite element modelling of fiber composites using a first order homogenization approach.

This report will map out the development and design choices during the design of the numerical tool. Using simple elasticity and plasticity material models for the constituents, a possible relationship between design parameters the stiffness and strength shall be investigated. The implementation of some damage criteria will be done to present the concept. A method for investigation into the effects of the different design parameters shall be explored by performing parameter sweeps.

1.4.1. Limitations

Environmental factors, fatigue, rate dependent aspects and impact of the structure may also be important factors which contribute to damage initiation, damage progression and failure in composite designs. While these factors should always be considered when designing against failure, they are not included as this is defined to be outside the scope of this thesis.

The results in this thesis is intended to demonstrate the modelling method, explore the method and investigate the effect of different design choices and design parameters. The results presented are based on simple material models and are not intended to accurately represent properties in fiber composites for design purposes. As fidelity of the estimations are not in focus, are common test like convergence due to element size not investigated. Before applying the developed tool in design cases, all results should be confirmed with experimental data with material models matching the composite constituents.

1.5. Structure of the Thesis

Based on the objectives, the thesis is organized as follows:

Chapter 2: Introduction of the relevant theory

Chapter 3: Explanation of the approach in detail and how the simulations were done to estimate the stiffness and strength in the RVEs.

Chapter 4: Estimation of linear elastic properties and the effect of different design choices and design parameters.

Chapter 5: The concept of multiaxial strength tests and failure envelopes and linear elastic stresses and strains for biaxial stresses.

Chapter 6: A strength testing approach through adjusting macrostrain with a backward iterative approach to maintain initial load case is investigated.

Chapter 7: Discussion of the produced results, validity and physical phenomena. Some results are briefly compared to estimations from other publications, approximations, failure criteria and normalized empirical data with ideas for further development.

Chapter 8: Conclusion

Chapter 9: References

2. Theory

In this chapter, the relevant theory of which the modelling method and simulations in this thesis are based on are briefly outlined.

2.1. Unidirectional fiber composites

Composites with unidirectional (UD) fibers as the reinforcement material show proportionally greater specific stiffness and strength along the fiber direction (González & Llorca, 2007). Therefore, UD fiber composites are used in a wide range of applications as structural materials for products like aircrafts, pressure vessels, automotive and wind turbine blades.

When applying UD fiber composites as structural materials in designs, a laminate configuration is common. These laminates are made by stacking thin layers of UD fibers, called plies, in different orientations into a layup before saturating the stack in a resin which hardens into the matrix material of the composite. The result is a single solid material which consist of several stacked UD fiber layers embedded in a matrix. In the manufacturing of such composites, the properties of the composite might be affected by several factors. Variations or differences in production methods, the properties of the constituents, volume fraction, shape and arrangement of the reinforcement in the matrix might lead to variations in the produced composites behaviour and properties.

When examining composites on the microscale, the arrangement of the fibers i.e. spatial distribution of the fibers in the microstructure will vary depending on the processing technique, melt flow index of the matrix, and parameters employed during the manufacturing process (Romanov et al., 2013). This indicates a random factor in how the fibers are distributed even though the same process is repeated.

Shrinkage of the matrix material during the curing process is an important aspect in manufacture. This process can cause the composite to develop residual stresses in the structure which affects the composites' strength.

To facilitate the stress transfer between the fiber and the matrix, fibers are often produced with a thin layer of hardened resin referred to as the sizing. Since fibers are produced goods there might be slight differences in fiber diameters and how successfully the sizing has been applied.

2.2. Constitutive relations

Hooke´s law is used to calculate the RVE deformations and stress states. Hooke's in the form of a material stiffness matrix as shown in equation ( )**Feil! Fant ikke referansekilden.** is used.

$$\begin{bmatrix}\sigma_1\\ \sigma_2\\ \sigma_3\\ \tau_{23}\\ \tau_{12}\\ \tau_{13}\end{bmatrix}=\begin{bmatrix}C_{11} & C_{12} & C_{13} & C_{14} & C_{15} & C_{16}\\ C_{21} & C_{22} & C_{23} & C_{24} & C_{25} & C_{26}\\ C_{31} & C_{32} & C_{33} & C_{34} & C_{35} & C_{36}\\ C_{41} & C_{42} & C_{43} & C_{44} & C_{45} & C_{46}\\ C_{51} & C_{52} & C_{53} & C_{54} & C_{55} & C_{56}\\ C_{61} & C_{62} & C_{63} & C_{64} & C_{65} & C_{66}\end{bmatrix}\begin{bmatrix}\varepsilon_1\\ \varepsilon_2\\ \varepsilon_3\\ \gamma_{23}\\ \gamma_{12}\\ \gamma_{13}\end{bmatrix} \quad (\ )$$

By applying single macro strains components (ε) to the RVE model the average stress state (σ) will be equal to the corresponding constants. By applying single strain components, each column in the matrix is estimated by measuring the average stress. The process for measuring the average stress state is described in the method chapter.

The elastic properties of a material are dependent on the geometry and the material properties. To estimate strength, an increasing load will be applied until failure. During the load case, the geometry of the RVE will deform. If nonlinear behaviour is assumed the stiffness constants will change as the RVE deforms. At the point of failure, the average stress is defined as the strength or ultimate tension/compression/shear stress.

Approximations

When approached analytically the geometry of UD composites on the microscale allows for the composite to be simplified to an orthotropic material, with three planes of symmetry, or a homogenous transversely isotropic material, with one plane of isotropy. An orthotropic material stiffness matrix is shown in equation ( ).

$$\begin{bmatrix}\sigma_1\\ \sigma_2\\ \sigma_3\\ \tau_{23}\\ \tau_{12}\\ \tau_{13}\end{bmatrix}=\begin{bmatrix}C_{11} & C_{12} & C_{13} & 0 & 0 & 0\\ C_{21} & C_{22} & C_{23} & 0 & 0 & 0\\ C_{31} & C_{32} & C_{33} & 0 & 0 & 0\\ 0 & 0 & 0 & C_{44} & 0 & 0\\ 0 & 0 & 0 & 0 & C_{55} & 0\\ 0 & 0 & 0 & 0 & 0 & C_{66}\end{bmatrix}\begin{bmatrix}\varepsilon_1\\ \varepsilon_2\\ \varepsilon_3\\ \gamma_{23}\\ \gamma_{12}\\ \gamma_{13}\end{bmatrix} \quad (\ )$$

While these approaches are useful for approximations, a real composite RVE might not have any of these idealized properties. Such assumptions can therefore not be made in the developed tool.

2.2.1. Micromechanical models

Stiffness models

Estimation of elastic constants when assuming composites as a transversely isotropic are done by calculating the constants of the stiffness matrix. By applying a rule of mixture, the stiffness constants for shear, transverse and parallel direction to the fibers can be approximated (Hull, 1981).

In the approximation for the fiber parallel elastic constant the error is usually between 1-2% (Hull, 1981). For the transverse elastic constants there is reasonable agreement, while shear constants approximations are usually not very accurate (Hull, 1981).

Strength models

According to González and Llorca (2007) the tensile and compressive strength of a composite in the fiber direction can be analytically estimated as the fiber and matrix behaviour closely follows the isostrain approximation. Analytical approximations of the mechanical behaviour under transverse loading are more difficult to approach.

When subjected to transverse loading, the composite behaviour diverges from isostress and isostrain behaviour and micromechanical models which are capable of predicting strength from factors like the constituents' properties, volume fraction and spatial distribution are not generally available (González & Llorca, 2007).

2.3. Modelling RVE geometry

To capture the geometric influence on the stiffness, a periodic RVE geometry is required. The information about fiber distribution and fiber radii in an RVE are described as that RVEs fiber population. Here, two methods of modelling a periodic fiber population are investigated. The first method is adjusting a realistic fiber population from picture recognition of microscopy. The second is generating close to realistic randomized fiber arrangements with an algorithm.

2.3.1. Describing composite RVE geometries

When observing an RVE, the information about numbers of fiber in the fiber population is easily observable. If the diameter of the fibers are known, and assumed to be equal, the fiber volume fraction is also easily calculated.

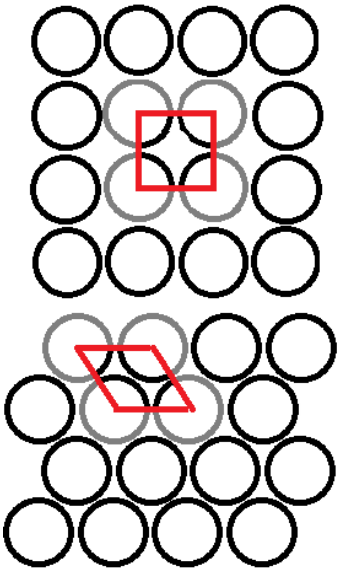

Figure 2.1: Periodic uniform fiber distributions

Specific fiber arrangement properties used when trying to describe an RVE are uniform distribution and periodic RVE, as illustrated in Figure 2.1. While these are highly descriptive terms, the fiber population of an empirical RVE is typically both non-uniform and non-periodic (Romanov et al., 2013).

RVE microscopic stress distribution is highly sensitive to the fiber distribution, while the macroscopic elastic effective response of a laminate may not be affected by it. Romanov et al. (2013) concludes that for an adequate prediction of the stress distribution on the micro-scale a realistic representation of fiber arrangements is required.

2.3.2. Critical RVE size

For an RVE to be able to sufficiently represent the whole microstructure, a certain size is required. For smaller RVEs, the representative material properties cannot be accurately estimated. While there is no universal way to estimate critical RVE size, critical RVE size has been measured as the number of fibers in the RVE. As shown by Swaminathan et al. (2005) in Figure 2.2: Plots showing convergence in the stiffness matrix constants as the numbers of fibers increase and deviation decease in the stiffness matrix constants as numbers of fibers increase. The researchers found 50 fibers to be a point convergence for the stiffness matrix. Regarding strength estimations there is not a significant difference between a 50 fiber and a 150 fiber RVE (Naya et al., 2017).

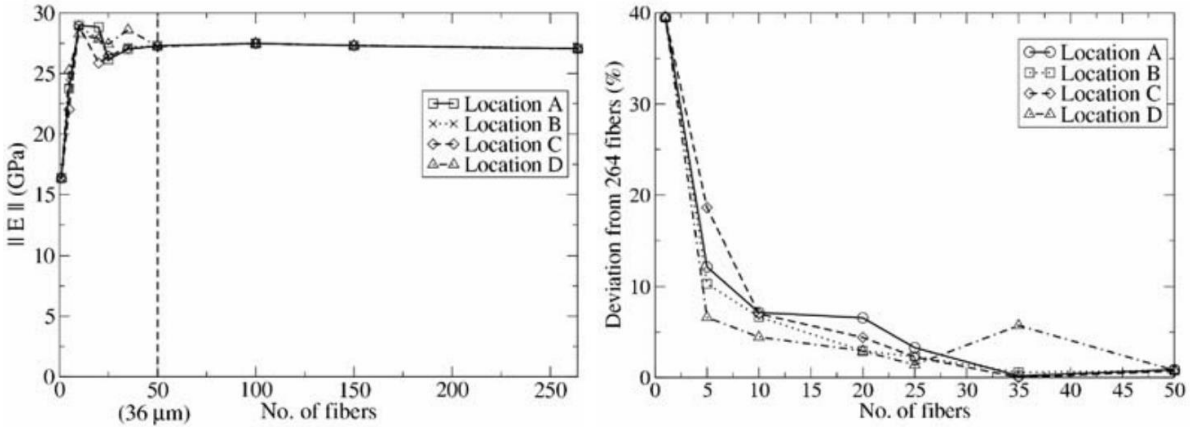

Figure 2.2: Plots showing convergence in the stiffness matrix constants as the numbers of fibers increase and deviation decease in the stiffness matrix constants as numbers of fibers increase.

2.3.3. Fiber Population

Romanov et al. (2013) states that the most straightforward way to find fiber populations is to use the fiber arrangement recorded from experimental composite samples. This is usually done by microscopy imaging of composite cross sections and ensures a realistic distribution in the fiber population.

While this method is effective for getting realistic RVEs geometries, the method is described as expensive and slow (Pulungan et al., 2017) and requires specific software for image recognition and equipment for microscopy. Nevertheless has a method using image recognition on black and white microscopy images successfully been applied to obtain the coordinates and radii of the fibers (Swaminathan et al., 2005).

A downside with realistic fiber populations is that they are rarely periodic. As mentioned on page 5, this is a challenge as periodic structures have proven to be the most versatile for modelling microstructures. While it is possible to adjust recorded fiber populations so they are

periodic, it might be necessary to do other adjustments as well due to FEA limitations. Given that the goal of this thesis is to model the RVEs in an FEA environment, some limitations of minimum inter-fiber distance apply.

Another approach Romanov, Lomov et al. (2013) suggest, is to simulate fibre distributions through a numerical algorithm. When generating a fiber distribution, the task is simplified to filling a square with small circles which do not overlap. By placing enough fibers, a given volume fraction of the area of an RVE can be reached.

Produced fiber composites have a practical max fiber volume fraction of around 65-75%. When using an algorithm which randomly places non overlapping fibers the algorithm usually stagnates for fibre volume fractions higher than 50-55 % (González & Llorca, 2007). As the practical maximum for the volume fraction in real composites are higher than this, methods for rearranging fibers can be applied to reach higher volume fraction values.

2.3.4. Statistically comparing generated RVEs to recorded fiber distributions.

Swaminathan et al. (2005) explain that a perfect RVE with precise representative values, according to the strictest definitions, may be impossible to simulate. The idea of statistically equivalent RVEs (SERVE) has therefore been proposed to identify whether a modelled RVE is a plausible realistic RVE and should be used to evaluate macroscopic homogenized properties in a microscopic analysis.

SERVEs can be identified as the smallest volume element of the microstructure which exhibits the following characteristics:

(i) The effective material properties, e.g., stress–strain behaviour in the SERVE should be equivalent to the properties of the entire microstructure, at least locally to a prescribed tolerance.

(ii) Distribution functions of parameters reflecting the local morphology, like local volume fraction, neighbour distance, or radial distributions, in the SERVE should be equivalent to those for the overall microstructure.

(iii) The SERVE chosen should be independent of the location in the local microstructure as well as of the applied loading direction, even for anisotropic material response.

(Swaminathan et al., 2005, p. 2)

Distribution functions of parameters reflecting the local morphology, like local volume fraction, neighbour distance, or radial distributions, in the RVE, should be equivalent to those for the overall microstructure to qualify as a SERVE.

Other methods used to statistically describe fiber distribution in RVEs include nearest neighbour distance and orientation, pair distribution function, radial distribution functions and Ripley's K function. Applying these in in a random algorithm models RVEs excludes certain fiber populations which may or may not be realistic.

2.4. Material models

The material effect of the RVE stiffness is based on material models for the different constituents. Some material properties are dependent on factors like time and temperature. Effects such as creep and relaxation are caused by the material reaction over time to the applied loads or displacements. Further are the constituents prone to several failure modes like micro buckling and brittle fracture in the fibers and cracking in the matrix.

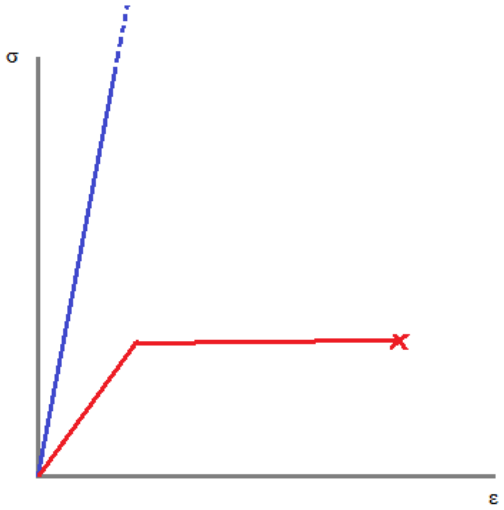

Figure 2.3: Simple elasticity and plasticity curves. The blue line models an elastic material and continues outside the graph. The red line, an elastic behaviour, then a plastic yielding until failure.

While some advanced material models can model failure modes like cracking, tension and compression hardening, the parameters in these advanced models can be difficult to obtain in experiments. When these advanced models are applied, these parameters are often iterated upon and calibrated to reflect macro experiments. Since advanced material models often are complex, the effects from the geometry and materials might be difficult to separate. To easily observe the effects of simple linear elastic and plastic behaviour, stress strain curves as in Figure 2.3 could be applied.

The type of stress variant used to decide effects like yield in an element will affect material behaviour. As Von Mises is the standard for isotropic materials in Abaqus, this was used in the plasticity models.

It is possible to assign several different damage models for matrix, interface and fibers. In this project simple damage models are applied. Matrix damage is modelled as a ductile maximum strain in the matrix, and delamination of the interface is modelled as a traction-separation degradation model for cohesive elements.

2.5. Finite Element Analysis/Method (FEA/FEM)

The finite element method (FEM) was used to model the RVE geometry, assign material properties and perform the simulations.

2.5.1. Modelling RVE constituents in FEA

When modelling the RVE, three different constituents are discretized: the matrix material, the fibers and the interface. The interface is found between the fiber and matrix material, and contains the sizing layer as shown in Figure 2.4. The interface is important in the stress transfer which is responsible of the reinforcing effect of fibres (Petersen, 2017).

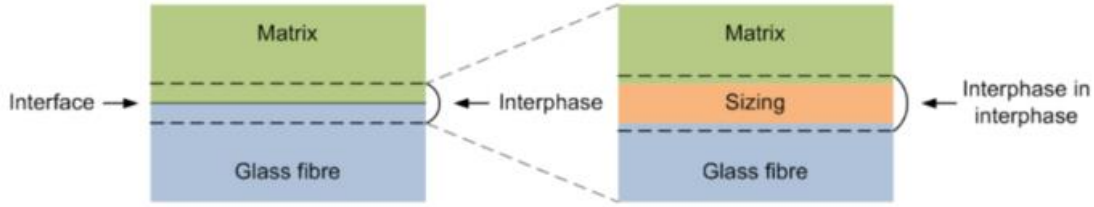

Figure 2.4: Sizing, the fiber matrix interface (Petersen, 2017)

The fibers and matrix geometry is defined in the fiber population and is easily divided into smaller elements in the FEA meshing of the RVE model. In the geometry of the sizing, the principle of separation of scales is challenged as this is much smaller than the RVE scale. The scale difference in the same model causes a problem with continuum mechanics.

One option is to model the RVEs without the interface between the two other constituent materials. This might affect stress transfer and will exclude the possibility of delamination between the fiber matrix.

The fibers were modelled with C3D6 elements and the matrix with C3D8R elements.

To model delamination in FEA two possible methods were investigated: modelling the interface as a cohesive surface or as a cohesive element (COH3D8) adhesive between the two components. These methods for modelling delamination were investigated:

- Cohesive surfaces. Infinitely thin layers inserted between the fiber and interface elements
- Cohesive elements. A special element type between the fiber and matrix

While both cohesive surface and the close to zero-thickness cohesive element can be used to model zeros thickness they return slightly different values.

2.5.2. Imposing macro strain

In the stress and strain simulations macro strains will be imposed on the periodic RVEs. The macrostrain is imposed as linear displacement. The periodic boundary conditions imply that for opposite surfaces, the deformation and the orientation are equal for stress continuity across the boundaries. At the opposite side of the RVE the stress vectors will be acting in the opposite direction. To apply periodic boundary conditions in FEA, constrain equations can be used to connect nodes on opposite boundaries. By defining a macro scale boundary value problem, which takes effect on the microscale, the structure displacements and micro stress distribution can be solved.

2.6. Simplified models

When simplifying problems, usually the estimates are affected. Simplifications often lead to one of two things: Either they assume details which can make the estimates return different values before and after the simplification, or they smooth over information that may affect the resolution of the estimate. As simplifications are a necessity in many simulations, the idea of consistent error is used.

When explaining consistent error, the difference between precision and accuracy becomes relevant. For a simulation which returns an estimate which is equal to the measurements from empirical tests, the simulation provides an accurate estimate. Nevertheless, a simulation does not necessarily need to return accurate results to be useful. Another possibility is that the estimates from a simulation are for example consistently proportionally different to the empirical measurements. Although the simulation is not accurate, the results have a consistent error relative to the accurate solution and can therefore be described as precise. The accurate values can be estimated from a precise estimation by adjusting for known consistent errors.

When creating a model for computer-aided testing with respect to strength and damage, it is still important that the model is complex enough to provide accurate and useful information about the phenomena investigated.

2.7. Monte Carlo methods

When creating a large amount of randomly generated fiber populations, each population can express either a plausible or an unrealistic fiber distribution. Although techniques to statistically test the fiber populations to find out whether they are plausible or not, these techniques are time consuming, might not filter away all unwanted fiber populations or might filter away interesting fiber populations. The estimations of material properties are therefore based on all created fiber populations.

As generating RVE models from all fiber populations creates scenarios that may or may not happen, a Monte Carlo method may be used to estimate the deterministic outputs of the randomness in the inputs.

Monte Carlo methods construct probabilistic models to describe real processes to estimate average characteristics. The effectiveness of Monte Carlo methods was first demonstrated by estimating pi. A number of points are pseudo randomly generated inside a square. Pi is then estimated by comparing the total number of points to the number of points which appeared inside a circle with the same diameter as the square sides, as illustrated in Figure 2.5.

Simply by using random sampling in the inputs to a mathematical model and then logging the results, the deterministic range of the output of the model can be determined. By using the random RVEs, and testing a large amount of these, an estimation for material capabilities regarding strength and damage can be made.

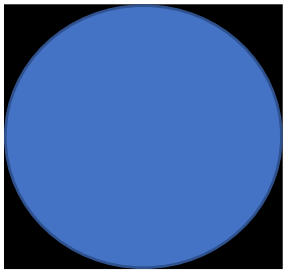

Figure 2.5: Pi estimated with a Monte Carlo method

3. Method

In this chapter the approach to the creation and testing of the RVE models are presented. First, the methods which were investigated to obtain a fiber population are described. Further, the material models applied to the RVE are introduced. The creation of the virtual RVE models in the FEA program is next, describing how the matrix, interface and fibers parts are modelled from a fiber populations and material models. To preform stress and strain tests a method of applying macrostrain to the model by constraint equations is presented with the procedure to extract the homogenised data.

3.1. Digital Environment

The FEA software Abaqus 6.14-4 was used to model and test the virtual RVEs as the software is provided by NTNU. The developed script which automates the process in Figure 3.1. The script was written in Python 2.7 with a structural programming approach.

For calculations and data handling, Python was used. The Python package Matplotlib was used for plotting results. The programming and script operations were performed in Pycharm 2017.3.1. Python 3.5.3 with the OpenCV package was used to investigate image recognition for obtaining fiber populations from microscopy.

To facilitate for repeatability the entirety of the code will be available for download with a setup tutorial at GitHub at a later date.

3.2. Overview of method

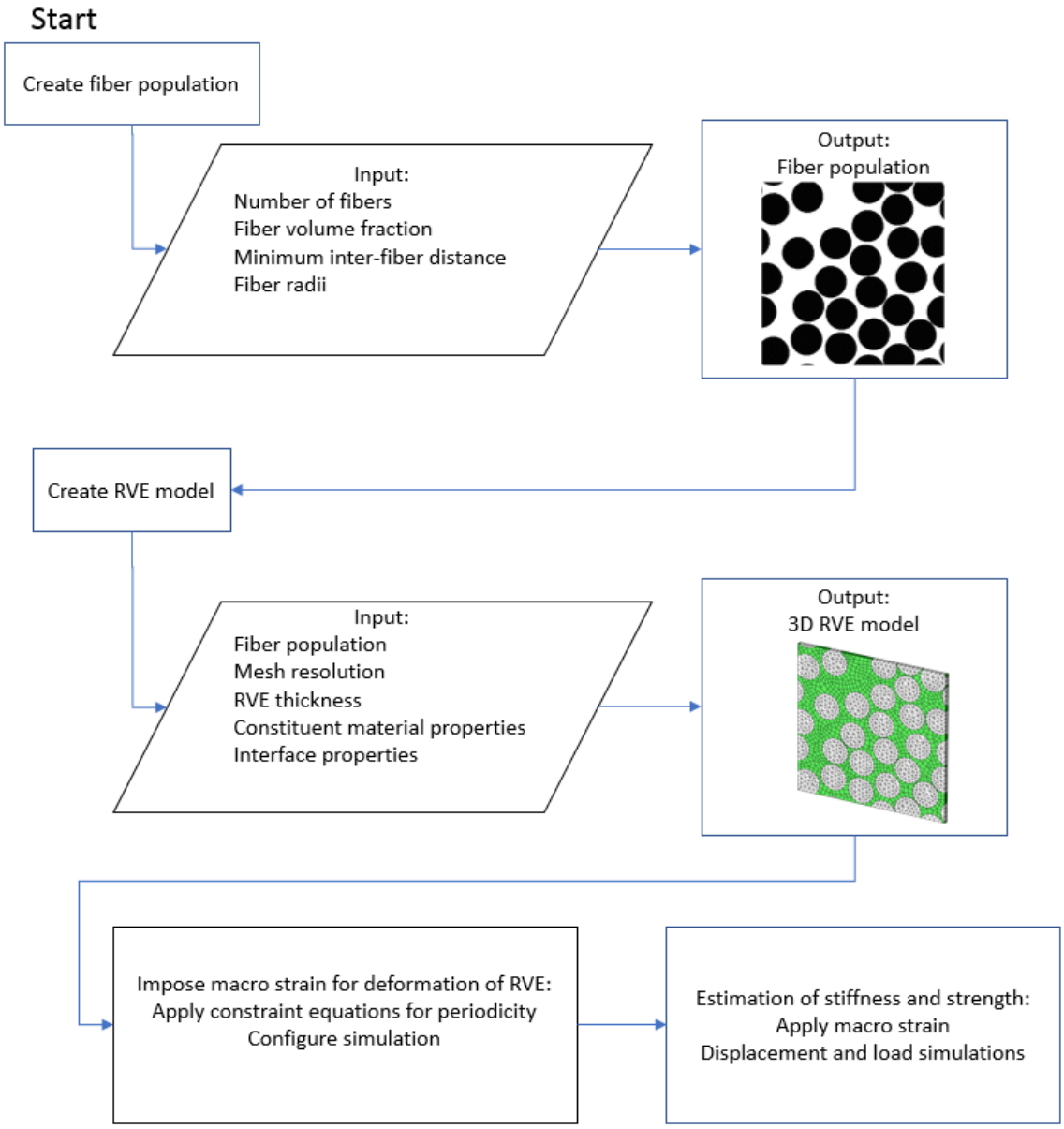

Figure 3.1: Flowchart for method

3.3. Finding fiber population

To model a fiber population, a reference fiber population must be found. Two ways of finding a fiber population are investigated: recording from real samples and simulating an arrangement. Both were tested with further research in mind and are presented in this section.

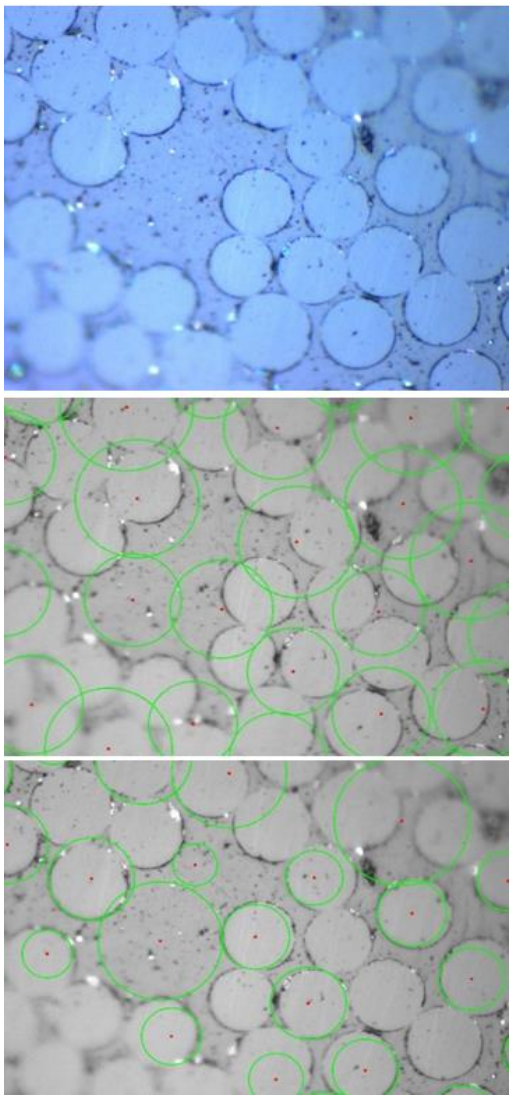

Figure 3.2: Circle recognition in a microscopy image with OPENCV.

Problem
Find fiber population

- Proposed solutions
  - Population from microscopy
  - Fiber placement algorithm
    - Toggles
      - Fiber variation
        - Parameters
          - Number of fibers
          - Fiber volume fraction
          - Fiber radii
          - Minimum clearing distance

3.3.1. Finding fiber population from microscopy image

Microscopy images were investigated by utilizing the OPENCV Python package for picture recognition. The image recognition software is based on the Hough Transform. The software scans the image looking for edges. Whenever an edge is found it is assumed to be a point in the outline of a circle. By rotating a circle around this edge point several times and incrementally increasing the radius while doing edge recognition for several other points in the circle, the circle is found.

The accuracy of the image recognition was found to be highly dependent on image sharpness and clarity. By editing the image contrast and establishing guiding parameters like expected diameter range for the fibers relative to the whole, image the software could make more accurate estimates. This method was quickly discarded as it either required consistent high

clarity microscopy images or a time-consuming calibration and visual inspection for each new image. Some attempts of circle recognition are shown in Figure 3.2.

3.3.2. Generating RVE fiber population

When generating fiber populations to model RVEs in a FEM environment there are a few aspects which are important to keep in mind. One aspect is what properties are intended for the RVEs, another is that FEM calculations introduce some limitations, like for example thin elements.

When imagining a repeating RVE as illustrated in Figure 1.3 it seems natural to model a periodic fiber population. To create this, the fibers at the edges or corners must be copied over to the other side to continue there as illustrated in Figure 1.5. This is done by placing another fiber on the oposite RVE border. In corner cases three extra fibers must be placed.

Thin elements might occur when the fiber edges are too close to the edge or in between two fibers. To avoid these, a minimum distance was enforced between fiber edges. This was done by adding half this distance to fiber radii when checking for overlaps.

Half this minimum distance was also enforced as the distance between fiber edges and borders. This was done by not allowing fiber centres to be in a dead zone, illustrated by the grey areas in Figure 3.3. This dead zone ensured that no fibers would create too thin elements on the other side.

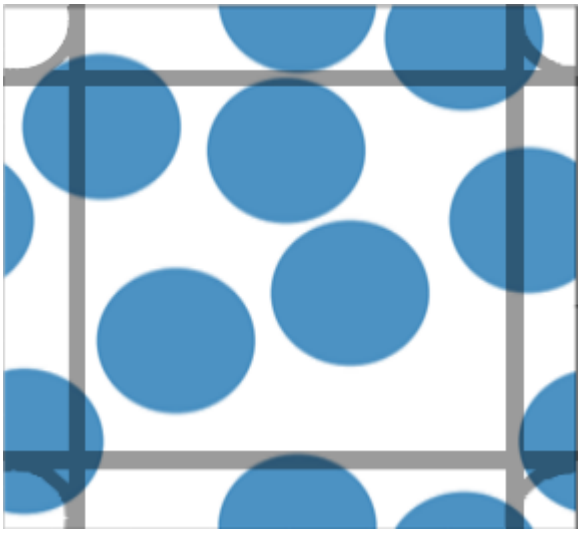

Figure 3.3: Fibers with the centre in the grey areas are discarded

As the distribution of fibers is inherently random, it seemed reasonable to generate random values for the fiber coordinates. Pythons pseudo random generator was used to generate the fiber coordinates. Pythons random generator is based on the Mersenne Twister method, which is a common random generator even though it is completely deterministic. The deterministic property assures repeatability as a given random key will generate the same random values every time.

The random generator generates a random number in the range 0 to 1. These generated values were multiplied with the size of the RVE to create fiber coordinates in the RVE.

3.3.3. Fiber variation

The effect of fiber size variation is investigated by adding the possibility of fiber radius variation in the fiber population generation. From still to be published work at the department an average fiber radius value with standard deviation is presented for a glass fiber population.

Fiber variation is implemented by assigning each individual fiber random radius generated from the mean and standard deviation before attempting to place the fiber in the fiber population. Due to the random assignment of radius the final fiber volume fraction in the populations can deviate some from the intended volume fraction. A 0.6 volume fraction in a ten-fiber fiber population may deviate up to around 10%. For larger populations this deviation is less.

3.3.4. Fiber placement algorithm

The fiber population function was created to be dependent on a small set of parameters: Fiber volume fraction (V_f), number of fibers (n_f) and fiber radius (r). From these values, the size of the square RVE (dL) was calculated through the V_f function. In this way r becomes a relative value to dL.

$$V_f = \frac{A_{Fibers}}{A_{Total}} = \frac{n_f \cdot r^2 \cdot \pi}{dL^2} \tag{3}$$

$$dL = \sqrt{\frac{n_f \cdot r^2 \cdot \pi}{V_f}} \tag{ }$$

The fiber adding algorithm used is illustrated in Figure 3.4.

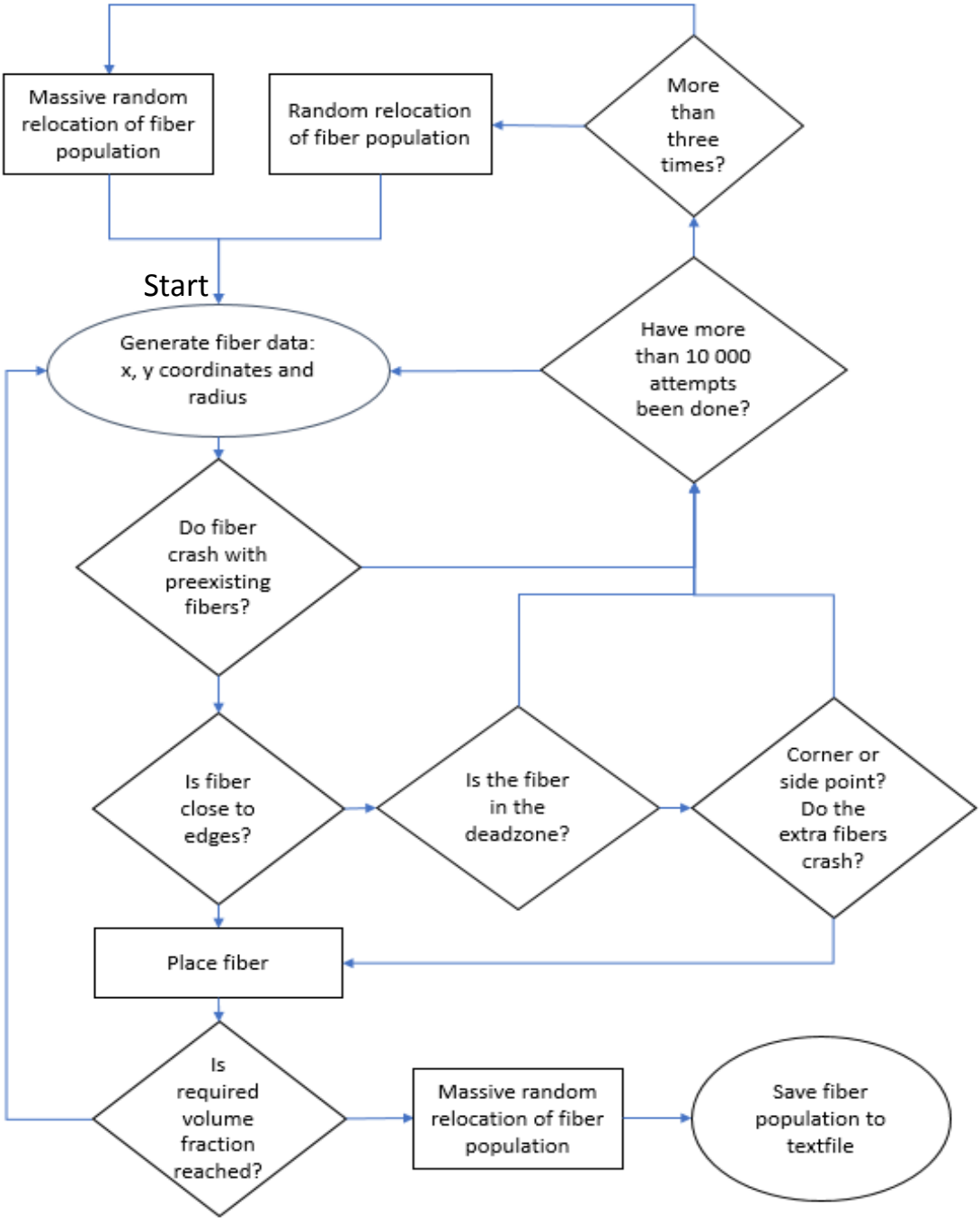

Figure 3.4: Fiber placement algorithm

A hard-code random algorithm is used until no more fibers can be placed. Then a fiber rearrangement function, which attempts to move the fiber centre to several new points within a set distance, is applied. The process of the relocation is illustrated in Figure 3.5.

The fiber rearrangement functions removes one fiber and tries to replace the fiber centre at a new location as illustrated in Figure 3.6. If this cannot be done within 20 attempts, the fiber is put back and the function moves on to the next fiber. For the standard random relocation each fiber is replaced as shown in the left illustration. If this fiber rearrangement function was tried tree times for all fibers without a new fiber being placed, another fiber rearrangement function is used. The rearrangement shown in the right illustration is then performed for all fibers, 20 times before the process continued. The massive relocation is intended to shake up the fiber distribution.

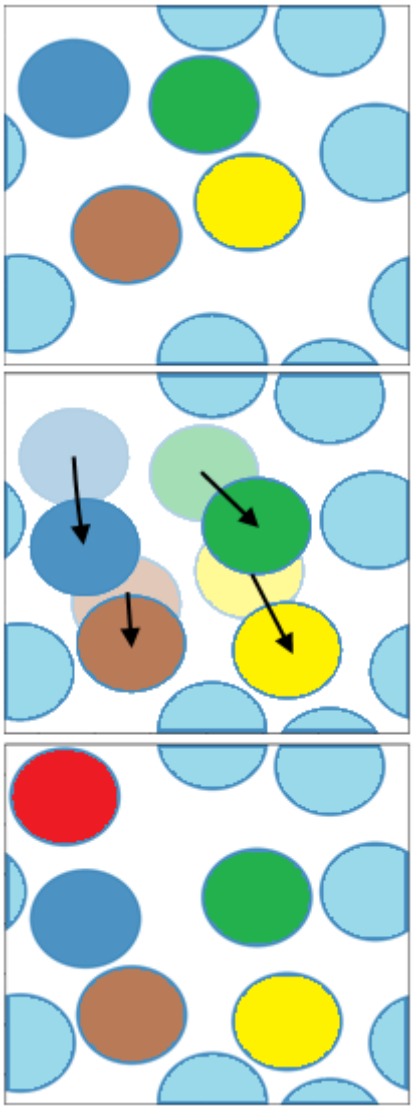

Figure 3.5: Rearrangement of fiber population

Initially, all fibers were replaced, including edge and corner fibers. This lead to the fiber distribution looking very uniform and made it possible to reach volume fractions over 0,85. To avoid the uniform appearance, the edge and corner fibers are now locked in place. The algorithm has still been able to reach volume fractions of 0,78 for RVEs above 30 fibers.

When sufficient fibers have been placed, the massive rearrangement function is performed several times for a final shake up of the fibers. The values of the design parameters are stored, and the fiber coordinates and fiber radii are written to text files for storage.

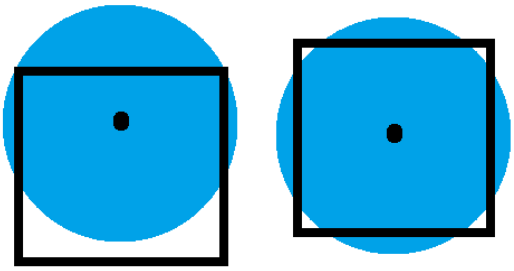

Figure 3.6: Fiber relocation window

3.3.5. **Validity of fiber populations**

Three possible descriptions for RVE geometries are used in this thesis: realistic, statistically plausible and modellable, as illustrated in Figure 3.7.

Due to practicalities, the modellable description of RVE's must be true. While the statistically plausible RVE geometries might ensure that the RVE geometries investigated are realistic, the application of these descriptions might filter out both modellable and realistic distributions. This might oversimplify the investigated fiber populations.

Therefore, all modellable generated RVE geometries were investigated. While the possible generation of unrealistic modellable RVE fiber populations might shift the estimations, the idea of consistent error may be applied to counter this.

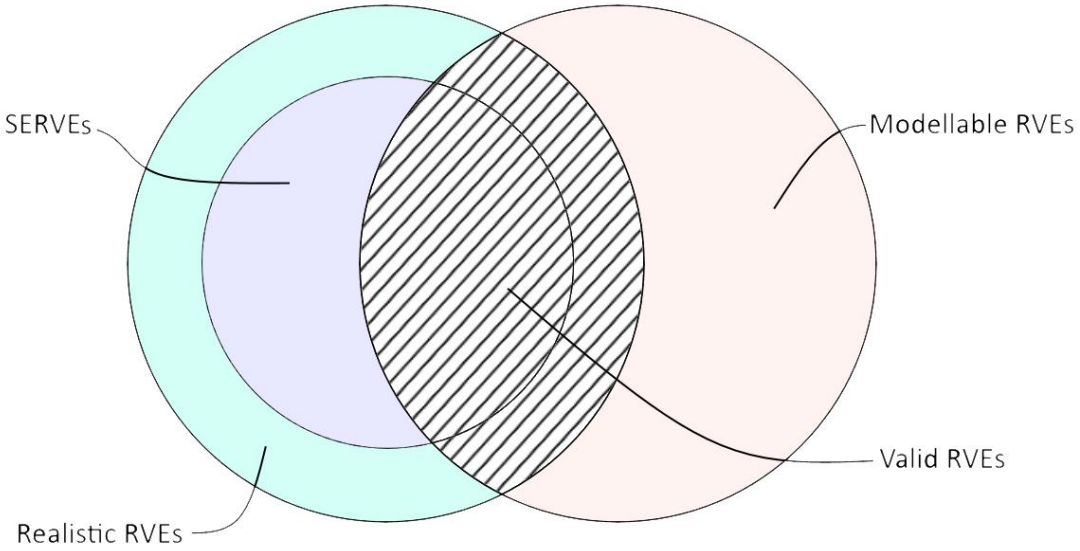

Figure 3.7: Validity of fiber populations

3.3.6. **Considerations**

While the hard-code random algorithm is quite straight forward, the fiber rearrangement can be done in several ways. Methods which actively try to place a new fiber by shifting other fibers, or creating open areas so new fibers can fit, could be applied. Since such strategic movements of fibers quickly get complex at tighter packing, the random method described was used due to its simplicity and efficiency.

3.4. Modelling RVEs

Problem
Create RVE model in FEA software

Proposed solution
Create 2D sketch, mesh and extrude mesh to 3D
Assign material models and element behaviour

Toggles
Interface
Fibers
Material models
Cohesive element type in interface

Parameters
Fiber population
Interface thickness
Mesh resolution
RVE thickness
Constituent material properties

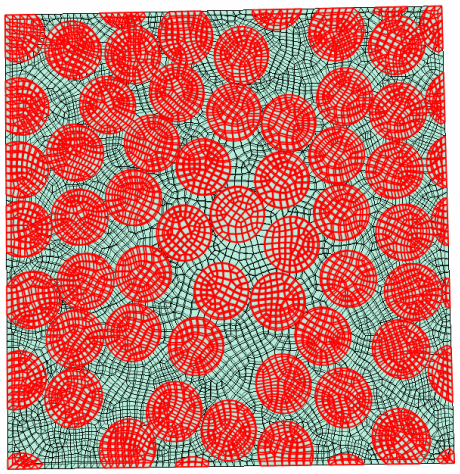

Figure 3.8: RVE model of composite microstructure

To create an RVE model in the FEA software, the generated fiber coordinates and radii were imported into the FEA and drawn onto a square 2D sketch with the same size as the RVE. The sketch of the fiber population was used to create a shell part which was meshed to a given mesh resolution and extruded into a 3D RVE of solid elements as shown in Figure 3.8. A method for modelling the interface as cohesive elements was explored by drawing another slightly larger circle around each fiber into the 2D sketch as illustrated in Figure 3.9. This allowed for the creation of interface elements around each fiber. The interface is present in Figure 3.8, but due to the size difference, not visible.

The thickness of the interfaces was set as a relative parameter to the mean fiber radii. To model the element thickness as zero, this parameter is set to be much smaller than any relative dimension (Dassult_Sysytems_Simula, 2014). The max interface thickness is limited by the minimum inter-fiber distance in the fiber population. This causes the interface to have a practical max thickness around ¼ of the inter-fiber distance to avoid thin elements between the interfaces. For higher mesh resolutions the

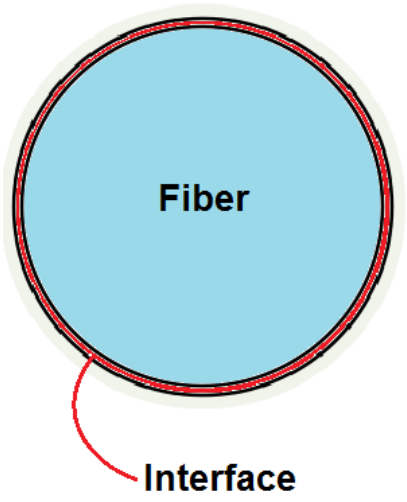

Figure 3.9: Fiber interface modelling

practical maximum tends towards ½ of the inter fiber distance.

While both cohesive elements and cohesive surfaces can be used to model zero thickness interfaces, they may return slightly different values (Dassult_Sysytems_Simula, 2014).

The mesh resolution or mesh element size is set by deciding how fine the circles should be in the model. The mean circumference of the fibers were divided by a required number segments around the fibers. In this way the element size is chosen as a fraction of the arclength. The extruded RVE thickness was set to be equal to the mesh element size.

The elements in the RVE models were divided into groups of interface elements, matrix elements and fiber elements. The different groups were then assigned different material properties.

3.5. Applying macro strains

Problem
Perform stable simulations

Proposed solution
Apply constraint equations to impose deformation

Parameters
Step size
Direction and magnitude of load or deformation

Kinetic constraint equations are used to maintain the periodic boundary condition of the RVE. By coupling the node pairs on opposite faces A and B to an external reference point outside the model periodicity and macro strains can be applied together. By then displacing the reference points the RVE border nodes are displaced. This allows for the possibility of applying compression, extension and shear strain.

For each degree of freedom, the following constraint equations are derived:

$$\begin{aligned}
\varepsilon_x &= \frac{\partial u_x}{\partial x} \Leftrightarrow u_x^b - u_x^a = \varepsilon_x (X^B - X^A) \\
\varepsilon_y &= \frac{\partial u_y}{\partial y} \Leftrightarrow u_y^b - u_y^a = \varepsilon_y (Y^B - Y^A) \\
\varepsilon_z &= \frac{\partial u_z}{\partial z} \Leftrightarrow u_z^b - u_z^a = \varepsilon_z (Z^B - Z^A)
\end{aligned} \tag{5}$$

$$\begin{aligned}
\gamma_{yz} &= \frac{\partial u_z}{\partial y} + \frac{\partial u_y}{\partial z} \Leftrightarrow u_z^b - u_z^a = \frac{1}{2}(Y^B - Y^A), u_y^b - u_y^a = \frac{1}{2}(Z^B - Z^A) \\
\gamma_{xy} &= \frac{\partial u_x}{\partial y} + \frac{\partial u_y}{\partial x} \Leftrightarrow u_x^b - u_x^a = \frac{1}{2}(Y^B - Y^A), u_y^b - u_y^a = \frac{1}{2}(X^B - X^A) \\
\gamma_{xz} &= \frac{\partial u_x}{\partial z} + \frac{\partial u_z}{\partial x} \Leftrightarrow u_x^b - u_x^a = \frac{1}{2}(Z^B - Z^A), u_z^b - u_z^a = \frac{1}{2}(X^B - X^A)
\end{aligned} \tag{ }$$

In equation (5) and (6) are the capital letters the initial node coordinates in x, y and z direction and u refers to the displacement of these nodes in the given degree of freedom.

As FEA calculate values at different frames, the parameters describing step size may affect the resolution of the calculated behaviour change in the simulation. For analyses estimating linear behaviour this is not relevant, but in nonlinear behaviour the step size should be small enough to capture relevant effects from the deformation on the stiffness components.

3.5.1. Considerations

The initial simulations were constantly aborted as the cohesive elements proved to be dependent on the element orientation. Cohesive elements model delamination between the element top and bottom surface. In the extrusion of the 2D shell the front of the 3D RVE was defined as the top. To model delamination between fiber and matrix the cohesive elements should have the top or bottom surface towards the fiber and the other to the matrix. To fix this the cohesive elements were deleted and reconstructed with the top towards the matrix.

In the process of identifying this error, techniques to create more stable simulations were investigated. This included applying boundary conditions to limit rigid body motion and assigning a very low viscosity to dampen the delamination in the interface (Gao and Bower 2004). While these methods were implemented in the script they were deactivated in the performed simulations after cohesive elements orientation were identified as the problem.

3.6. Stiffness prediction

For estimation of elastic properties, linear behaviour is modelled. To find the stiffness matrix for the RVE, single component macro strains were imposed on the RVE model. This way the average stresses which develop due to the imposed strain will be equal to one of the columns in the stiffness matrix.

The average stresses were calculated as shown in equation ( ):

$$\bar{\boldsymbol{\sigma}} = \frac{1}{V}\sum_i \boldsymbol{\sigma}_i V_i \tag{7}$$

For each element the stress components were multiplied with the element volume. The element centroid stresses (measured stresses in the middle of each element) were used for the calculations. The sum of these where then divided by the sum of all element volumes.

3.7. Strength prediction

In strength estimations non linear RVE behavior for a load case should be simulated. As the simulations work by imposing macro strain Hooke's law in equation (8) is used. By inverting the stiffness matrix, the compliance matrix is found. By deciding load cases the corresponding macro strains can be found by multiplying the stresses with the compliance matrix. By applying these strains, the RVE will be subjected to this load case.

$$\begin{bmatrix} \varepsilon_1 \\ \varepsilon_2 \\ \varepsilon_3 \\ \gamma_{23} \\ \gamma_{12} \\ \gamma_{13} \end{bmatrix} = \begin{bmatrix} S_{11} & S_{12} & S_{13} & S_{14} & S_{15} & S_{16} \\ S_{21} & S_{22} & S_{23} & S_{24} & S_{25} & S_{26} \\ S_{31} & S_{32} & S_{33} & S_{34} & S_{35} & S_{36} \\ S_{41} & S_{42} & S_{43} & S_{44} & S_{45} & S_{46} \\ S_{51} & S_{52} & S_{53} & S_{54} & S_{55} & S_{56} \\ S_{61} & S_{62} & S_{63} & S_{64} & S_{65} & S_{66} \end{bmatrix} \begin{bmatrix} \sigma_1 \\ 0 \\ 0 \\ 0 \\ 0 \\ 0 \end{bmatrix} \quad (8)$$

The same approach as described in 3.6 was used to calculate the average stresses.

When an RVE model is tested for strength a load case with nonlinear behaviour is imposed to cause deformations in the RVEs. As stiffness is based on geometry and material properties the stiffness will change as the deformation manifests.

3.7.1. Backward iterative macrostrains adjustment

The initial load case was maintained through a backward iterative approach. By identifying at what frame in the simulations the average stress components diverge from the initial load case the point of divergance is found. To find the adjustment, the change the in average stresses between the diviation frame and the previous frame creates a gradient for each stress component. The gratidents for the stress components for the loadcase are set to zero as these are the ones being investigated. The rest of the stress gradients are scaled to the remainder of the test after the diverging frame. This way expected stress divergence values are quantified.

Even though the initial stiffness matrix changes thorughout the load case it is still a reference to the RVE stiffness matrix. Therefore this was used to find the corresponding macro strain values to the stress divergence. After the strains were updated the simulation was restarted from before the divergion to continue the initial load case. The process was repeated until the simulation was complete, or the values diverged too much due to the RVE stiffness constants having changed from the deformation.

Before this method was developed, a single strain component adjustment method and a method for finding the Jacobian was explored. Both methods requiered multiple iterations before any progress was made in the simulations.

Another approach to do pure load tests is by using Abaqus user subroutines. While this approach is expected to improve the process it was not explored due to little experience with the Fortran programming languange.

3.8. Summary of design parameters

The design parameters the following modelling and simulations were based on are presented here. Unless explicitly stated the properties in the simulations are as presented here. In some simulations the parameters are changed to investigate the effects of these parameters.

Constituent material properties

The fiber is modelled as an isotropic material with elastic behaviour. The Youngs modulus and Possion ratio of the fiber material are 70 GPa and 0.2.

The matrix material is modelled as an isotropic material with an elastic behaviour followed by a plastic yield. The Youngs modulus and Possion ratio of the elastic behaviour are 3.0 GPa and 0.35. The matrix yield limit was set to 0.06 Gpa. The interface is modelled as an elastic isotropic adhesive with the same Youngs modulous as the matrix.

Matrix damage is modelled as a simple maximum strain of 0.035 for ductile metals with a close to instant damage evolution. The delamination is modelled as traction-seperation damage of the cohesive elements with damage initation at 0.061 GPa with the quadric nominal stress criterion. The damage evolution of the cohesive elemetns is a linear softening behaviour with the fracture energy parameter set to 0.0078.

Geometry parameters

The fiber variation was set to have a mean fiber radius of 8.7096 with a standard deviation of 0.6374. The data was provided from still to be published data from the department.

For all simulations a fiber volume fraction of 0.6 is used unless otherwise stated.

The minimum clearing distance between fibers was set to be 2% of the fiber radius mean unless otherwise stated.

Simulation parameters

The mesh size used in all simulations was stated as a fraction of the average fiber circumference. A resolution of 25 elements around the fibers was used for all simulations.

To perform stable simulations, no strain components in the macro strains exceed 0.15. The simulations step size was automatically calculated by Abaqus with an initial step size of 1/100.

4. Part 1 - Estimation of linear elastic properties and parameter effect

In this chapter, linear behaviour is simulated to investigate elastic properties in the RVE models. When assuming linear behaviour, the stiffness matrix stays constant. To illustrate how design parameters effect estimations, an example of a parameter investigation will be given.

To investigate the effects of different design parameters, it is necessary to get consistent estimations of the linear elastic properties of RVEs. Due to this, tests to estimate the critical RVE size and required number of samples to reach convergence was made. This test was done to get a benchmark of the effect of different fiber populations before investigating the effects of the design parameters. As the required RVE size and number of samples for the other tests were based on this benchmark, the results are presented before the other tests are described.

4.1. Effect of fiber distribution on different RVE's sizes

Swaminathan et al. (2005) found that when testing stiffness in smaller RVEs, the results deviate from properties found for RVEs of a certain size. By combining this with the approach of several random generated RVEs to estimate an average, the following hypothesis was formed:

The average of the stiffness matrix constants for several RVE's based on different fiber populations converges to the same value independently of RVE size. The accumulated average of the stiffness constants converges faster for larger RVEs due to less scatter in the larger RVE stiffness constants.

Simulations

To investigate stiffness convergence for different RVE sizes, 100 simulations based on different random keys were done for each test. The different tests investigated RVE models based on 5 to 59 fibers with nine fiber intervals in RVE size, resulting in seven tests with 100 simulations. The limitation to seven tests is due to computational power. A high-end computer today, with eight CPU cores, can run seven simulations simultaneously without freezing.

The convergence of the stiffness components is investigated by finding the accumulated average for each component of the stiffness matrix. While there is no guarantee whether the RVE will reach convergence within 100 tests, a trend might become visible. From 100 samples, a mean and standard deviation with some statistical significance can be found.

4.1.1. Results.

The results are presented in the following figures. In Figure 4.1 the deviation of the stiffness matrix constants as the RVE size increases are presented. Figure 4.2 and Figure 4.3 show the convergence of the stiffness matrix constants for the different sized RVEs. The first graph of Figure 4.2 shows the elastic constant in fiber direction. The second graph presents the transverse constants. In Figure 4.3, the convergence of the shear and coupling constants are shown. The stiffness matrix of a single 10 fiber RVE is quantified in equation (9) for reference.

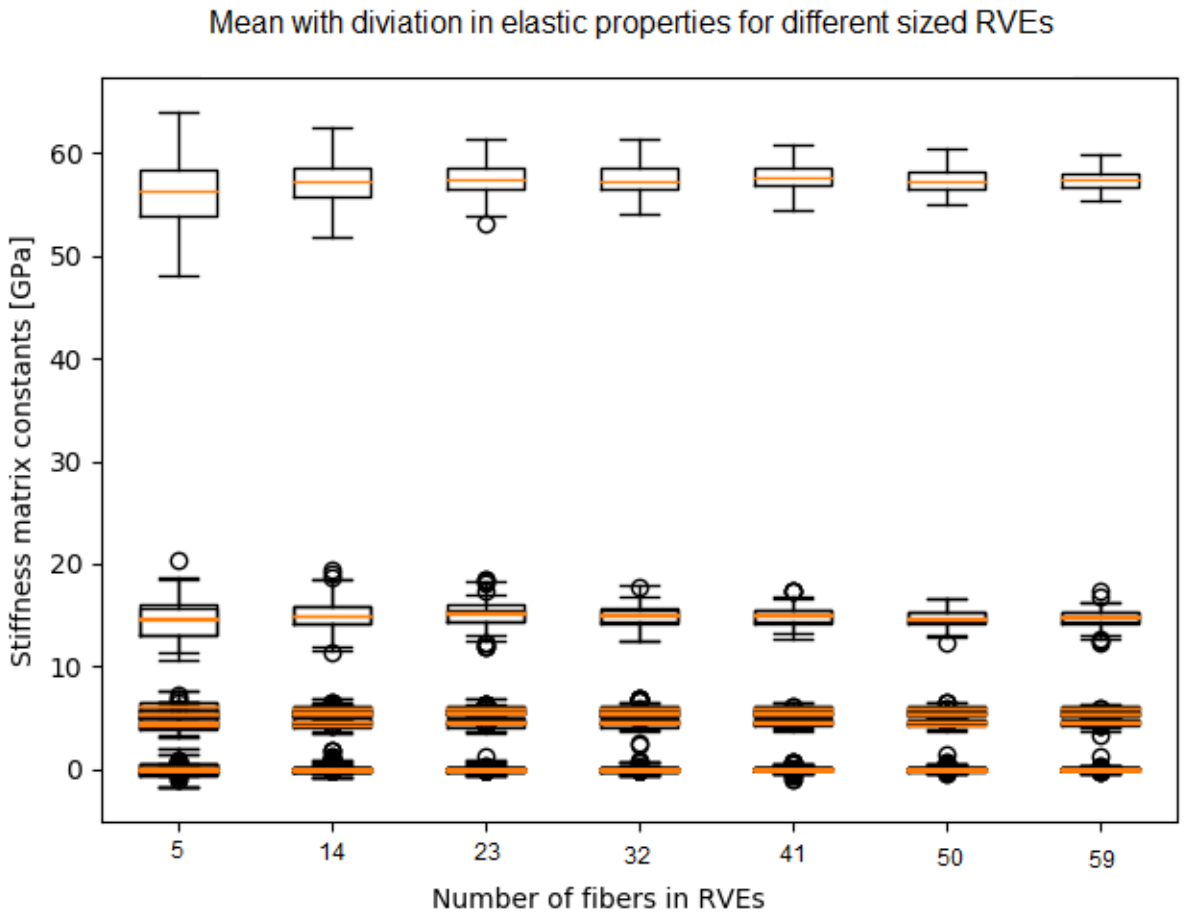

Figure 4.1: Elastic properties for different RVE sizes.

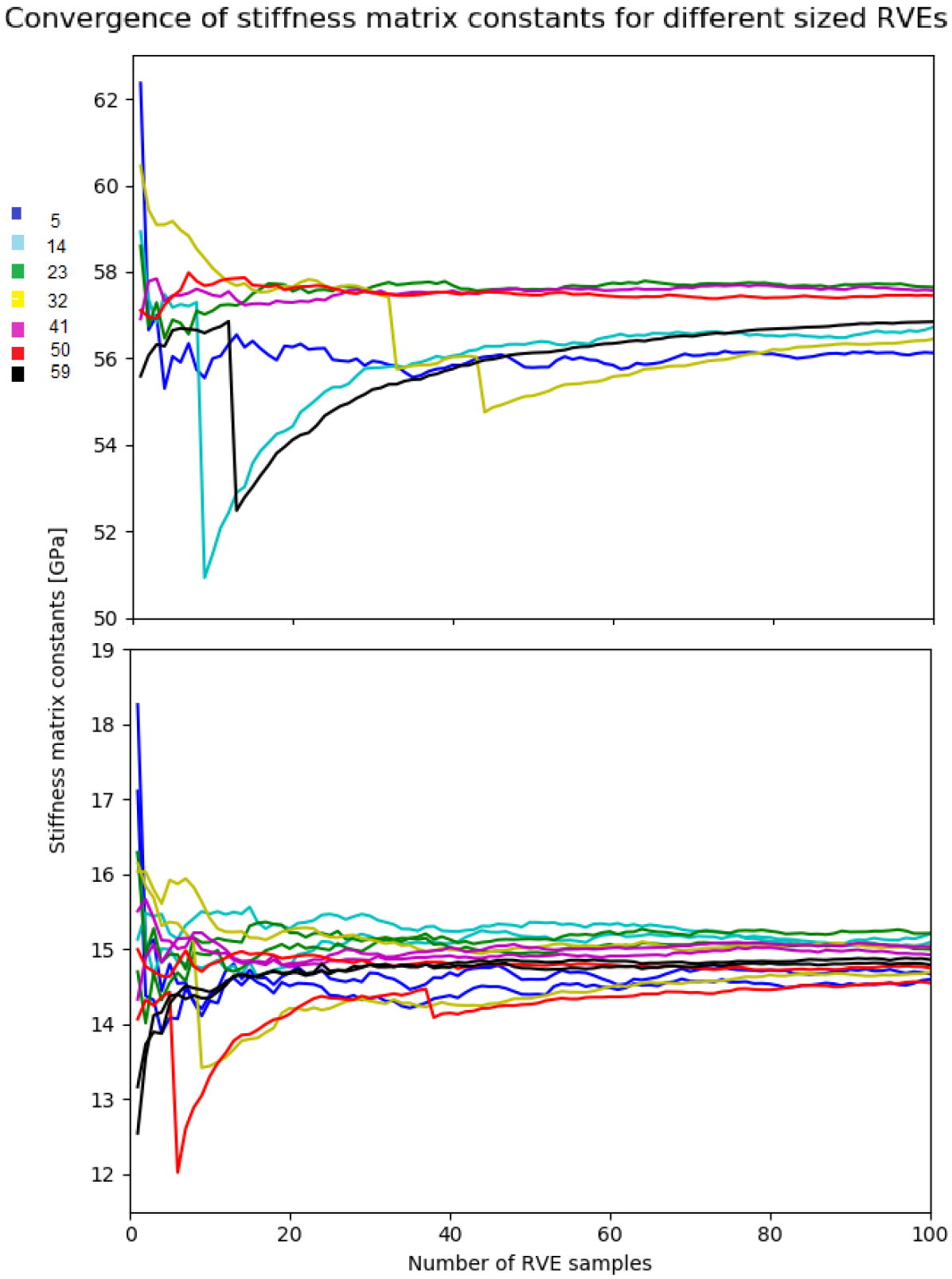

Figure 4.2: Fiber parallel and transverse constants

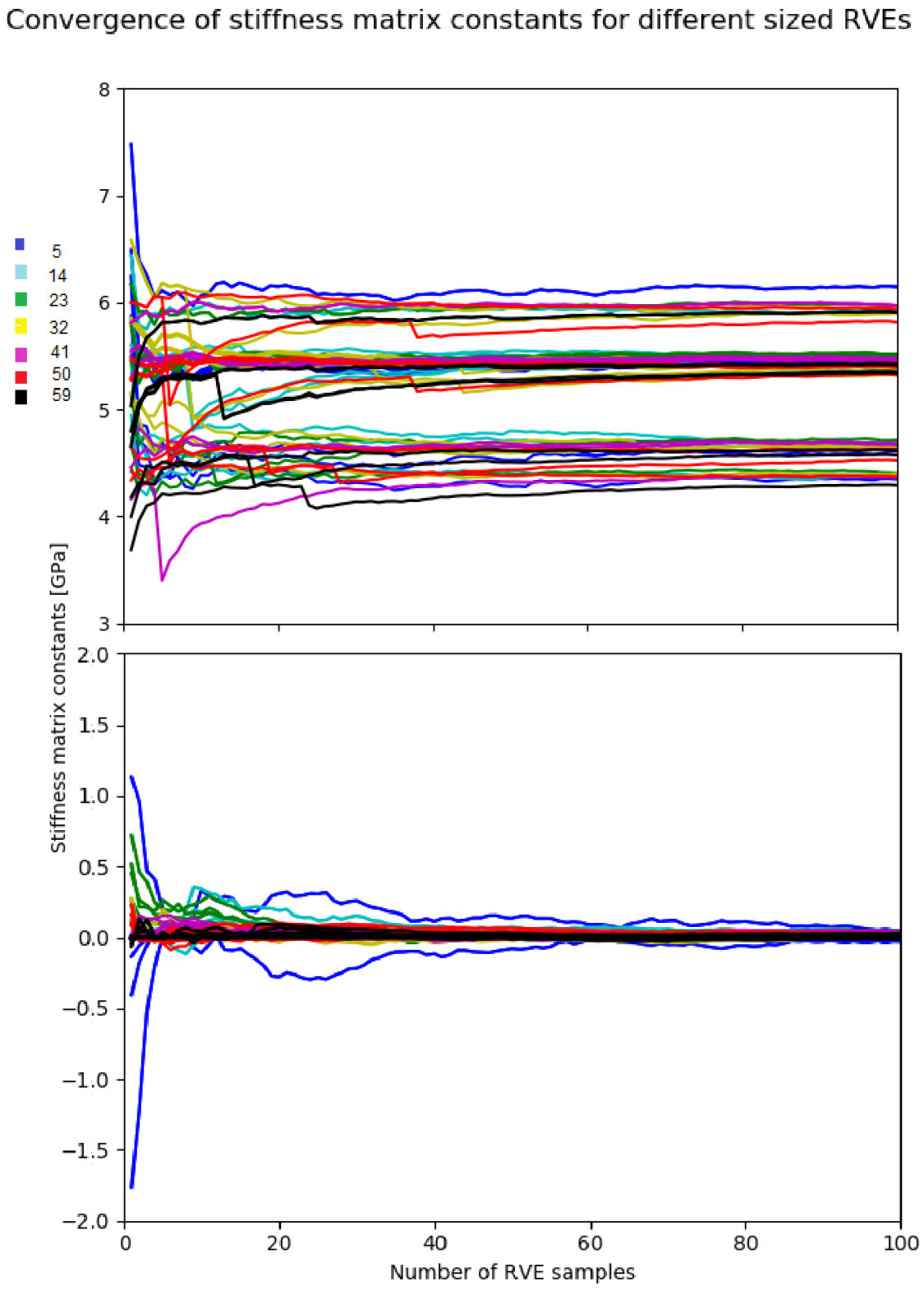

Figure 4.3: Shear and coupling stiffness constants

While the exact value of convergence for the stiffness matrix constants are not identical for the different RVE sizes, they all seem to tend towards a similar value. In the following parameter investigations RVE models with 25 fibers were used. While this size seems to overestimate some properties, this value was chosen as a compromise between time and

accuracy. The same compromise was made for the number of simulations in the test. 50 RVE samples, based on different random keys, were used in each test while the convergence only stabilizes after about 80 samples. If a clear effect of the parameter change is visible within this number of tests the parameter change is presumed to affect the linear properties.

4.2. Effect of geometric parameters on elastic properties

Fiber volume fraction

The stiffness approximations mentioned in 2.2.1 are based on the rule of mixture, which are dependent on the constituents' volume fraction. The changing of the fiber volume fraction is therefore expected to affect the stiffness matrix constants.

Generally higher fiber volume fractions show higher stiffness matrix constants. Seven tests were performed to investigate the effect of raising the volume fractions from 0.4 to 0.7 with 0.05 increments.

Minimum clearing distance

As the fiber placement algorithm is designed to place fibers with a certain minimum inter-fiber distance, the effect of the scale of this distance was investigated. Two tests to investigate the effect of changing the minimum distance from 0.5% to 5% of the mean fiber radius were done. Smaller minimum distances between fibers are expected to cause greater stresses which could cause higher stiffness.

Effect of fiber variation on elastic properties

The effect of modelling fiber variations was investigated by performing two similar tests with and without the fiber variation option. In one test all the fibers were given the same radius. In the other tests, the fiber variation was as described in 3.8.

4.3. Effect of interface on elastic properties

After a fiber population was created, it was used as the basis for an RVE model. To investigate the effect of modelling an interface, a single fiber population was investigated with different modelling choices and parameters.

Effect of modelling interface

To investigate whether the modelling of the interface in the RVE has any effect on the elastic properties, the stiffness was estimated with and without cohesive elements between the fiber and matrix. The interface elements were assigned matrix material properties.

Effect of interface properties

The interface element thickness was increased to a practical max size, ¼ of the minimum inter-fiber distance 0.02. For the tests, the interface elastic modulus and yield limit was first set as 100 times higher, and then 100 times lower compared the resin properties. These values are chosen to model a much stronger interface and a much weaker interface relative to the matrix.

4.4. Result of geometric parameter investigations

Fiber volume fraction

In Figure 4.5 and Figure 4.4, one can observe that the fiber volume fraction affects the stiffness matrix constants. In Figure 4.5, the change in elastic properties in the fiber- and transverse directions is found to increase as the fiber volume fraction increases. In Figure 4.4, the shear and coupling effects from Figure 4.5 are shown at an enlarged scale. The shear stiffness constants are also found to increase as the fiber volume increases. The increased volume fraction also causes a higher deviation in all constants.

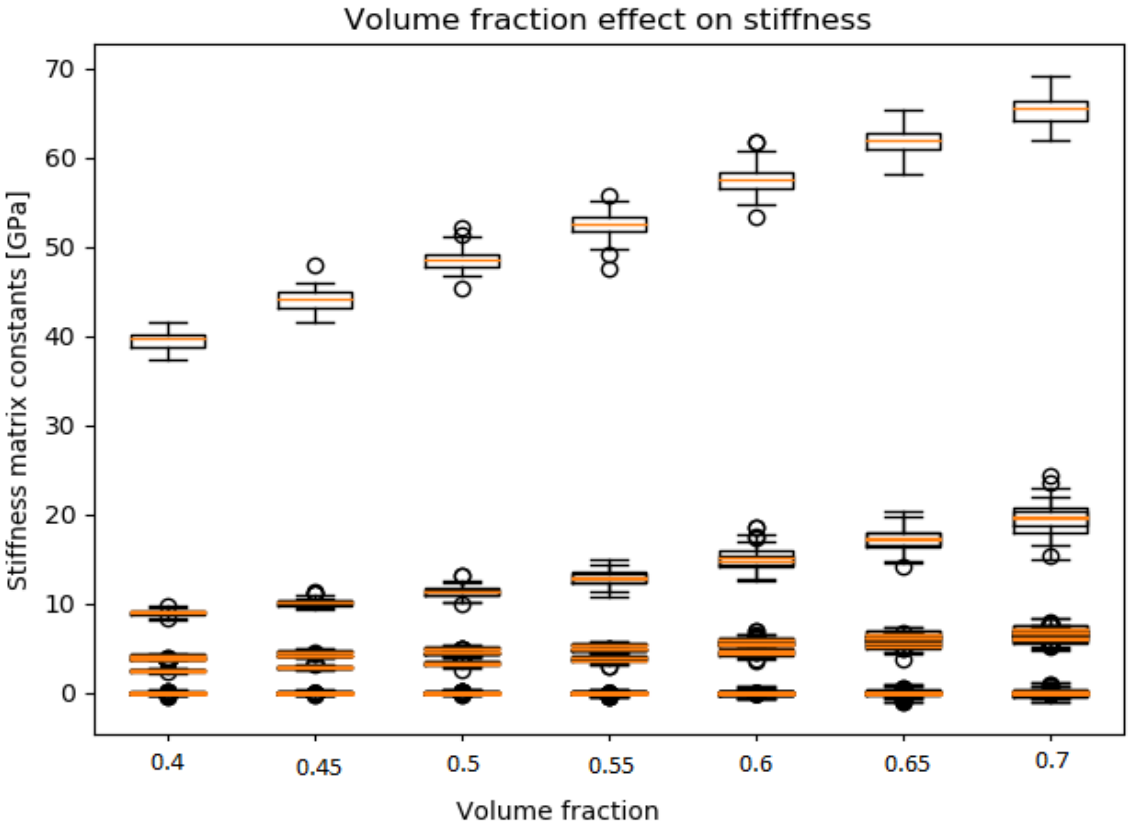

Figure 4.5: Stiffness constants for different volume fractions

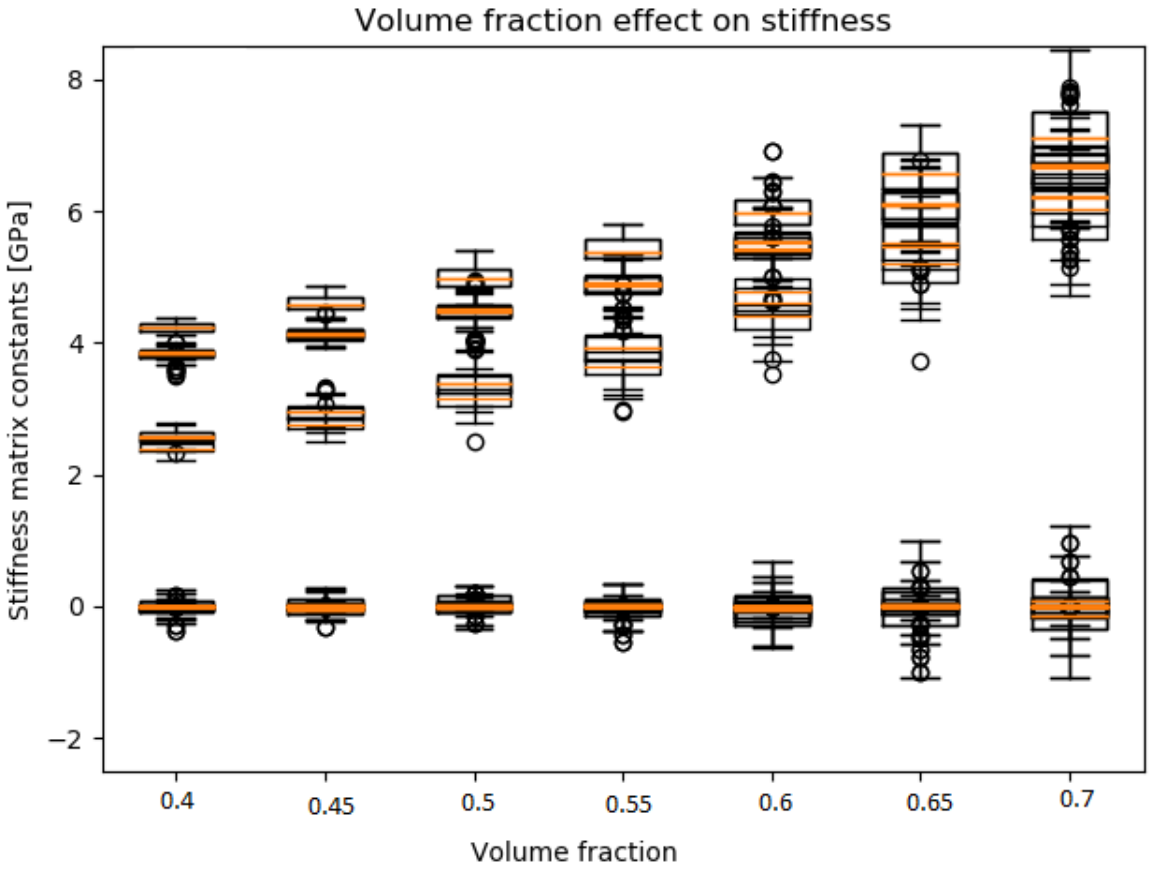

Figure 4.4: Shear and coupling stiffness constants of different volume fractions

Minimum clearing distance

In Figure 4.6, it seems like the deviation increases for smaller inter-fiber minimum distances. A further examination of the scale of the different stiffness matrix constants are presented in Figure 4.7. In the top left plot of this figure, the fiber parallel stiffness constant is presented and the transverse constants are below. The top right plot shows the shear constants and the bottom right, the coupling constants. From these figures, it seems that the stiffness matrix constants for parallel, transverse and shear directions, slightly increases for larger minimum inter- fiber distances.

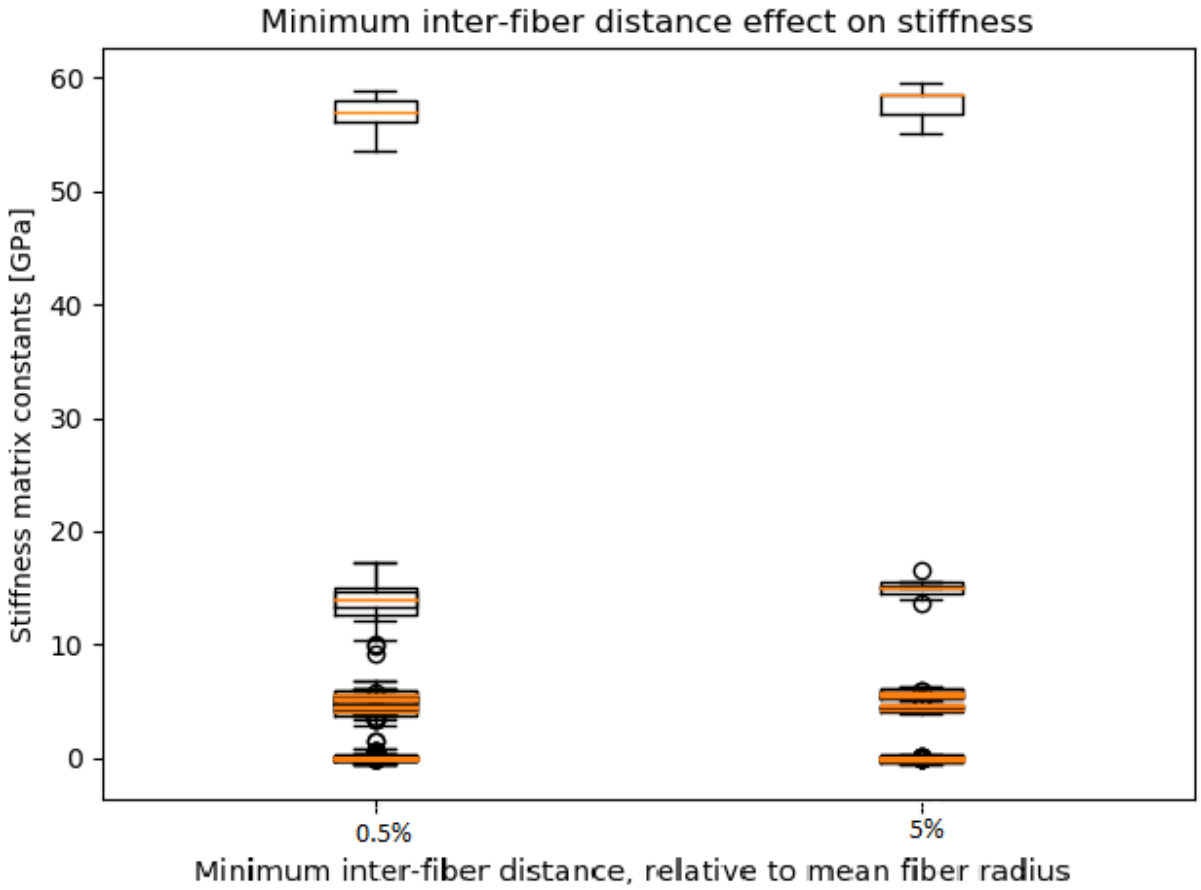

Figure 4.6: Effect of minimum clearing distance 1

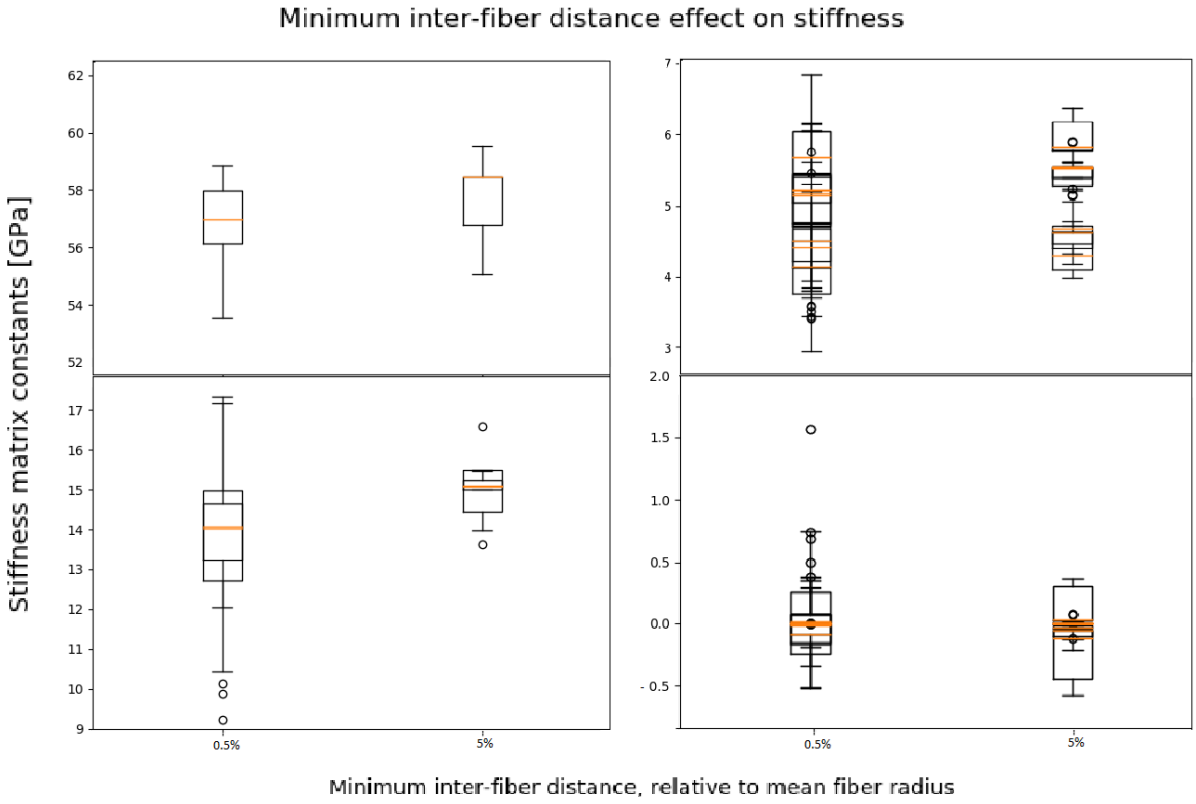

Figure 4.7: Effect of minimum clearing distance 2

Effect of fiber variation on elastic properties

Figure 4.8 shows that the modelling of fiber variation in the fiber populations has an effect. The stiffness constants for the RVE models with fiber variation are found to deviate more than the constants for the RVE models without fiber variation. Some of this deviation is due to the fiber variation option introducing some deviation in the volume fraction. There also seem to be a slight difference in the converged values.

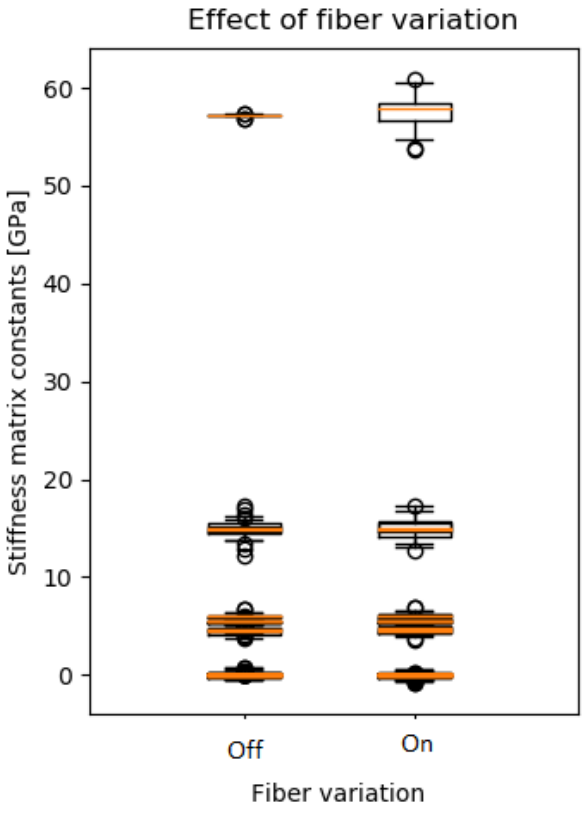

Figure 4.8: Effect of fiber variation

4.5. Results of interface options

Effect of modelling interface

The effect of modelling of an RVE with and without the cohesive interface elements on the different stiffness constants, are plotted in Figure 4.9. The fiber parallel constant seems to be somewhat lower for the RVE without the cohesive interface. For the transverse and shear constants the values are somewhat higher without the interface.

While the coupling constants are changing slightly with the interface toggling, the effects seem quite insignificant. In all cases the differences in constants are less than the converge scatter in test 4.1.

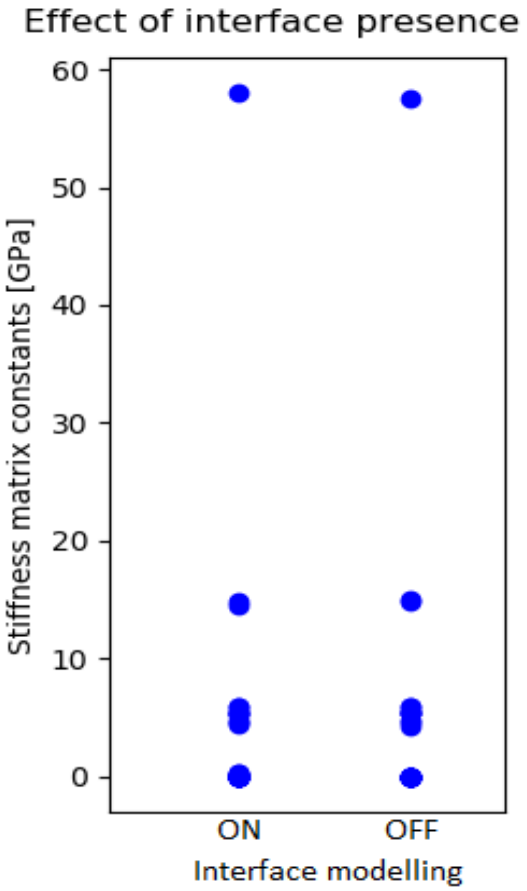

Figure 4.9: Effect of interface modelling

Effect of interface properties

The changes in the interface elastic modulus and yield limit influenced the elastic properties of the composite. From Figure 4.10, it seems that the upscaling of interface properties slightly increases the fiber parallel, transverse and shear constants compared to Figure 4.9. The fiber parallel constant is not very affected. The downscaling of the interface properties affects the transverse and shear constants a significant amount. The coupling constants are also changing with the interface changes, but these effects seems to be insignificant. The changes in fiber parallel and coupling constants are less than the converge scatter in test 4.1.

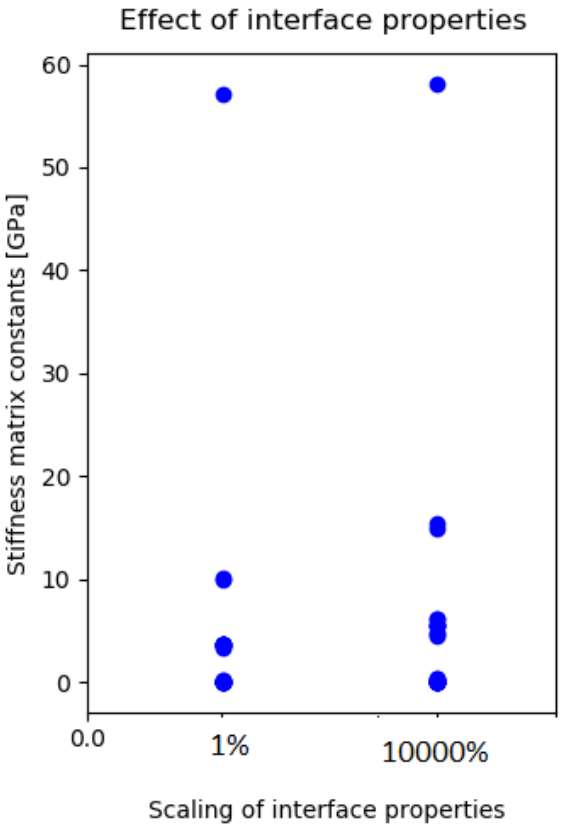

Figure 4.10: Effect of interface properties

5. Part 2 - Linear elastic exploration of load cases

This chapter explores stress testing through imposing macro strains on the RVE models. The approach is here applied on linear behaviour. This allows for exploration of possible load cases and introduction of the concept of failure envelopes or lotuses through quick linear simulations.

5.1. Bi axial stress sweeps for initial stress distribution

Hooke's law is used to find the matching macro strains required to do different load cases. When investigating biaxial load cases, the loads can be imposed in many possible proportions and directions. An approach of choosing normalized load cases based on different stress components, as illustrated in Figure 5.1, is applied to sweep through several possible biaxial load cases. The approach can be done for any two stress components. All possible combinations of biaxial load cases can be investigated for several different load proportions.

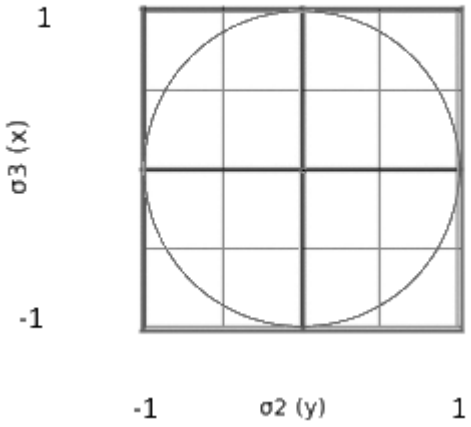

Figure 5.1: Possible normalized biaxial load cases

The stress values of the elements are presented through many different stress variants and can be extracted from the elements in the RVE. Abaqus offers several different stress variants which provides different information.

5.1.1. Test

Transverse-transverse load cases were investigated. 180 possible load cases equally spaced around Figure 5.1 were done. With this level of resolution, the tension-tension, compression-compression and tension-compression cases will be thoroughly investigated. The max stress value in the elements was extracted from the matrix for each load case and inversed to get the load proportionality factor for this load case.

Several stress variants were extracted and a few of these are presented below. The fiber populations of the tested RVE models had 50 fibers. To consider the effect of fiber

populations, three different RVE's were tested. The small number of tests is because chapter 5 is deemed as a brief intro to nonlinear testing addressed in chapter 6, and not a more thorough investigation as in chapter 4.

5.2. Linear envelope results

Von Mises

Figure 5.2 shows the load proportionality envelopes for the Von Mises stress variant in σ_2-σ_3.

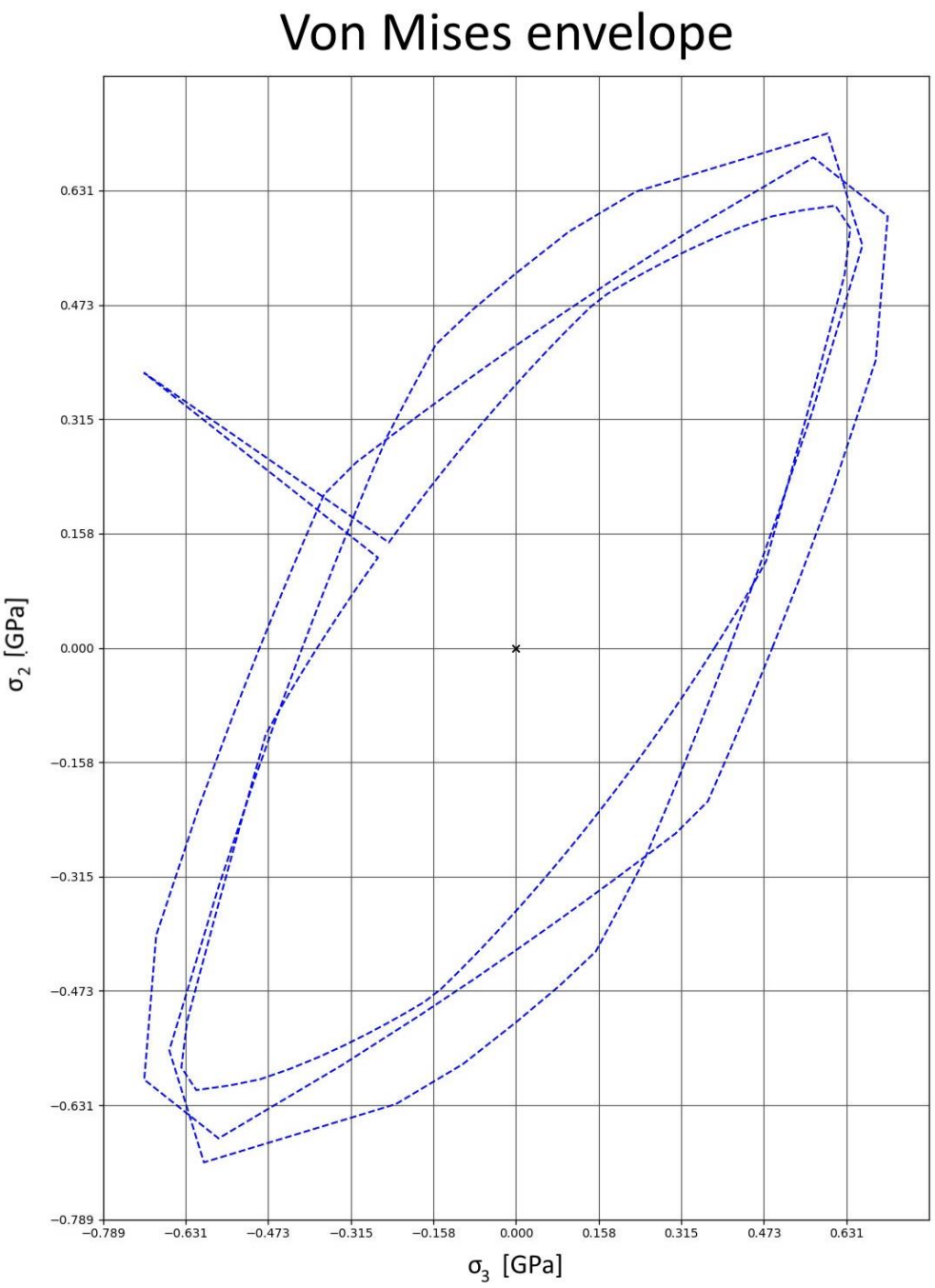

Figure 5.2: Initial Von Mises stress envelope for biaxial loads

Max principal stress and strain

In Figure 5.3 are the load proportionality envelopes for the max principal stress variant in σ_2-σ_3 load cases shown. The values at the 45-degree tension-tension state differ noticeably.

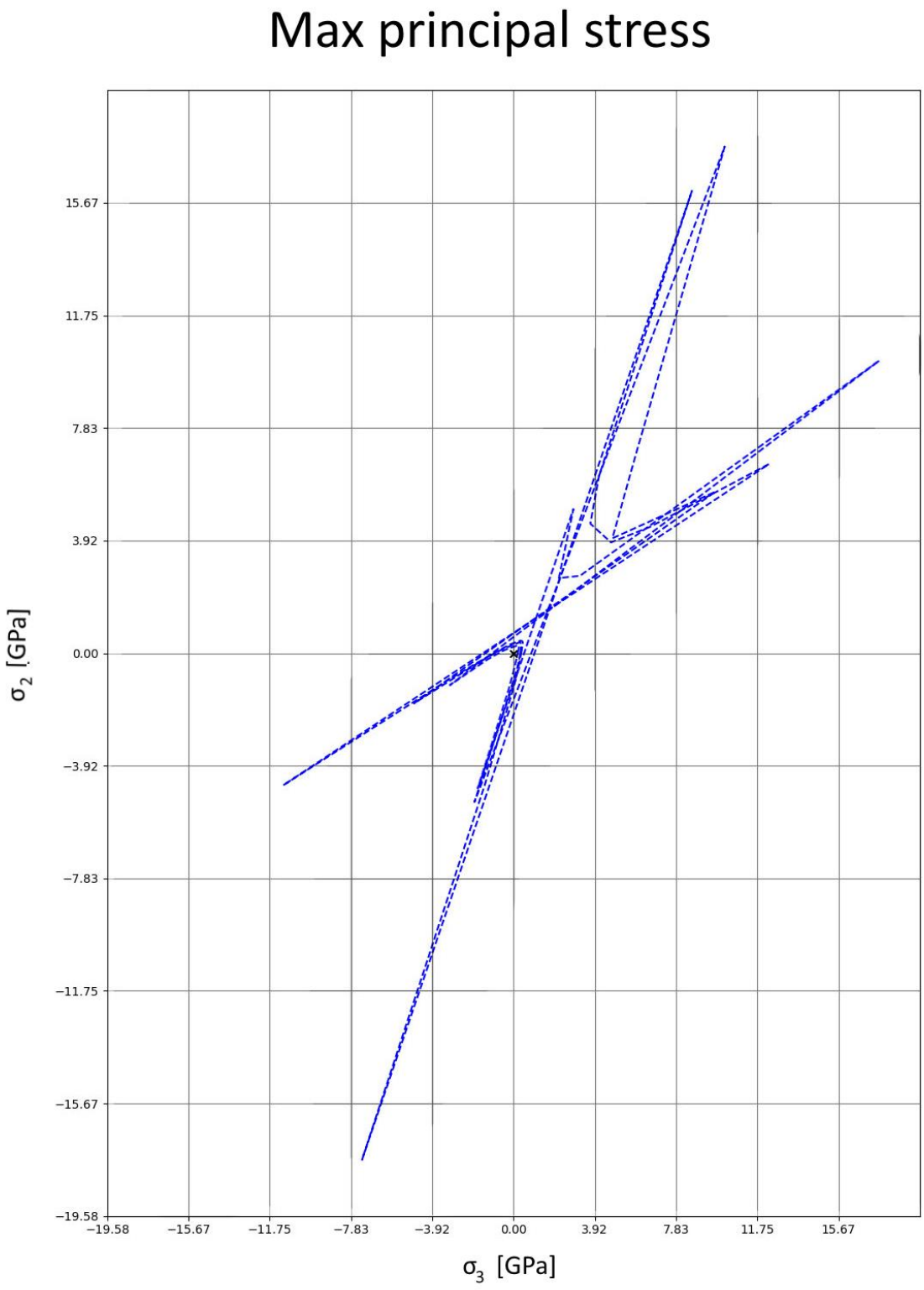

Figure 5.3: Initial max principal stress for biaxial loads

Figure 5.4 shows the load proportionality envelopes for the max principal strain variant for the σ_2-σ_3 cases.

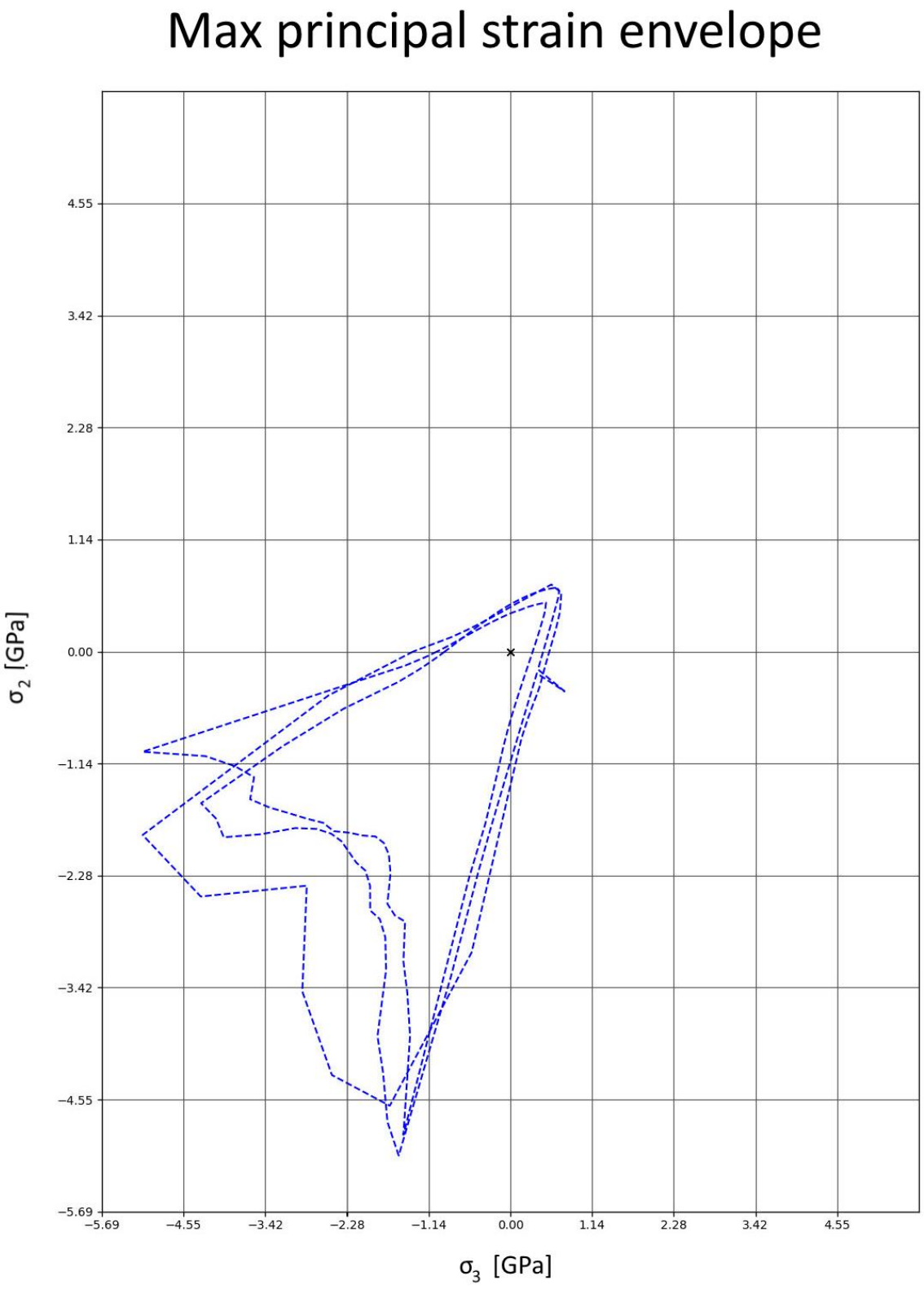

Figure 5.4: Initial max principal strain for biaxial loads

Max Shear stress and strain

In the next two figures, Figure 5.5 and Figure 5.6, are the load proportionality envelopes for the max shear stress and max shear strain variants presented. In one of the max shear strain cases the envelope did not plot properly, due to poor scaling of the axes in addition to several spikes. The result of this RVE is not plotted.

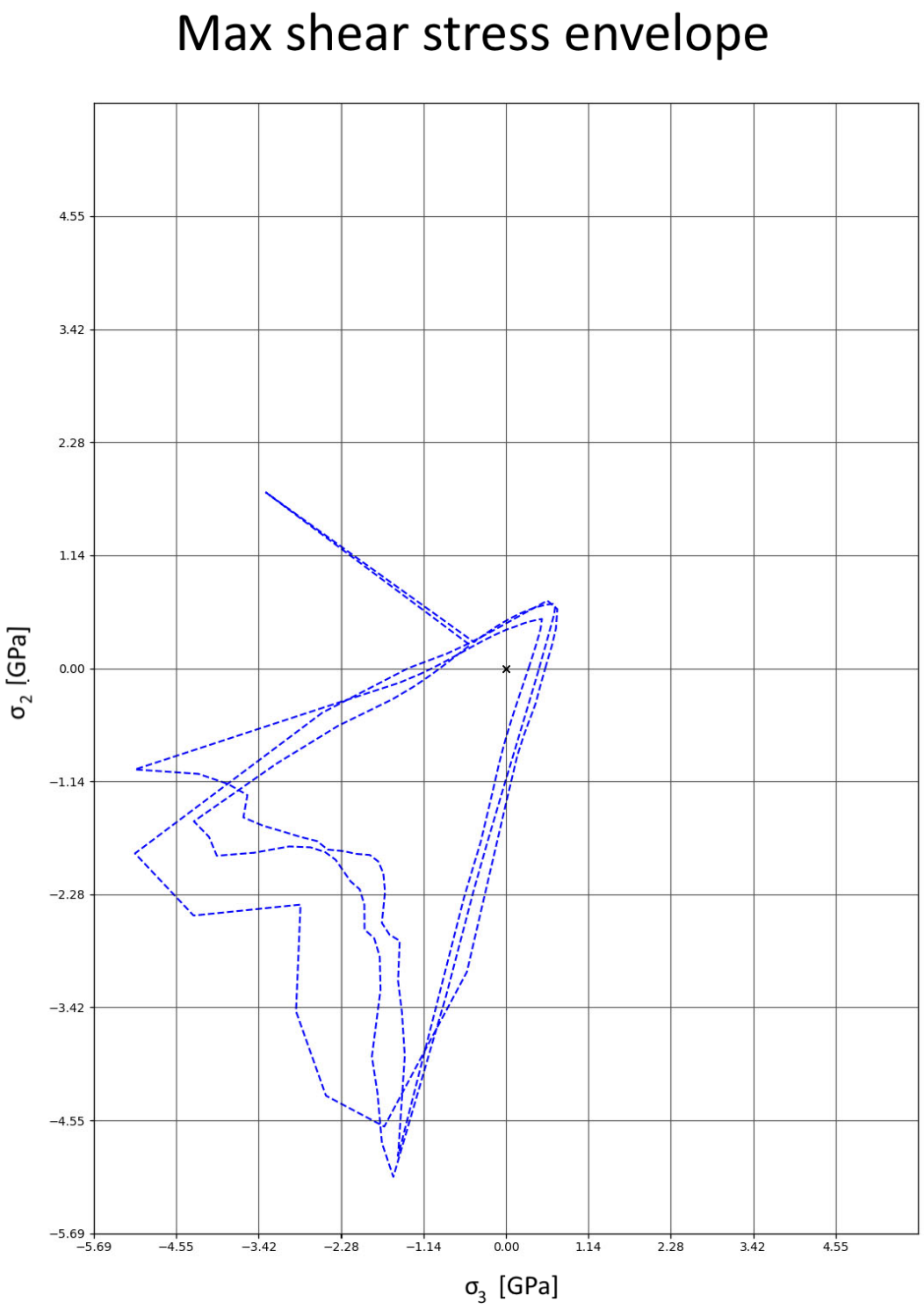

Figure 5.5 : Initial max shear stress for biaxial loads

Figure 5.6: Initial max shear strain for biaxial loads

6. Part 3 – Nonlinear behaviour

In this chapter stress testing on RVE models with nonlinear behaviour is explored. In the first part is plasticity, fracture strain damage and interface degradation material models introduced to demonstrate the effects of these different material models.

In the next part are biaxial stress tests introduced and transverse-transverse tests performed. From the transverse nonlinear tests is a failure envelope, based on a small number of tests, created.

As some of the stress states on the different simulations are found to deviate from the initial load case, a backward iterative method is explored to maintain initial load case as explained in 3.7 Strength Prediction.

6.1. Material models

Plasticity models

Nonlinear behaviour with plasticity material models as explained in 3.8 is tested. As this test does not include any damage, large deformation as illustrated in Figure 6.1, is possible. This level of deformation is far from realistic in composites. Because the fibers are modelled as a linear elastic, and the matrix as an elastic plastic material, little hinders the deformation in these simulations.

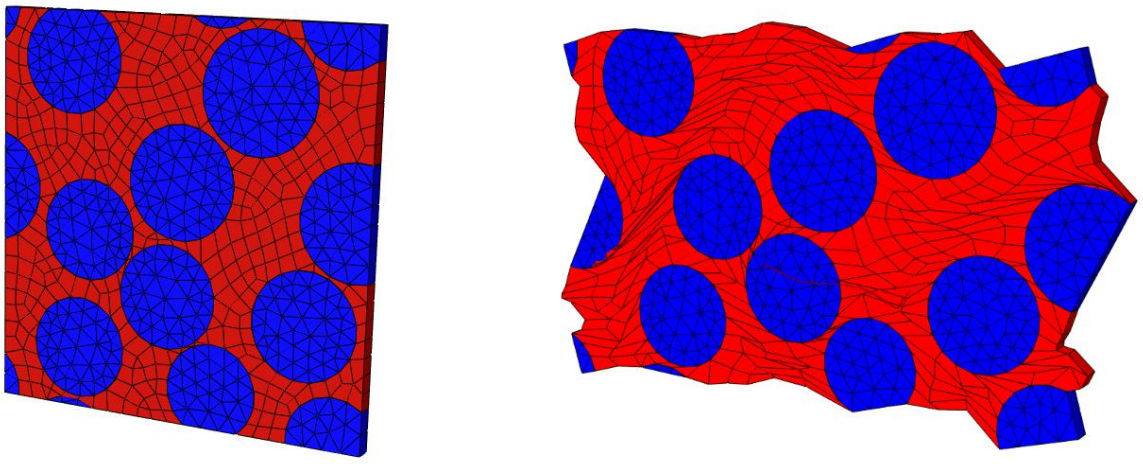

Figure 6.1: A transverse macrostrain intended to stretch the plastic RVE by ~20%

Plasticity and Matrix damage

To demonstrate damage modelling in the matrix, a simple max strain ductile damage model is added to the matrix elements to determine when the matrix elements breaks. This testing does not consider other damage and failure modes so the results may still be far from realistic. The tests are primarily intended to demonstrate a matrix damage model.

Plasticity, matrix damage and cohesive.

Delamination in the interface elements are modelled as described in 3.8. Now both the matrix and interface elements are assigned different simple damage models. The strength estimations are now based on interface degradation and matrix damage.

6.1.1. Simulations

All tests were done with nonlinear stress simulations on a single ten-fiber RVE model as larger RVEs have a longer simulation time. The small RVE size might present inaccurate values, so the following tests are only intended as a demonstration of the method. The stiffness matrix of the tested RVE was found to be as in equation (9).

$$\boldsymbol{\sigma} = \begin{bmatrix} 53.814 & 5.359 & 4.938 & 0.109 & 0.000 & 0.000 \\ 5.342 & 14.454 & 5.945 & 0.405 & 0.000 & 0.000 \\ 4.924 & 5.946 & 12.478 & 0.106 & 0.000 & 0.000 \\ 0.108 & 0.405 & 0.106 & 4.199 & 0.000 & 0.000 \\ 0.000 & 0.000 & 0.000 & 0.000 & 4.624 & 0.244 \\ 0.000 & 0.000 & 0.000 & 0.000 & 0.245 & 3.884 \end{bmatrix} \boldsymbol{\varepsilon} \tag{9}$$

The imposed macro strains were calculated as follow: by assigning a strain value to a single strain component, a corresponding stress state is calculated through the stiffness matrix. The other stress components were then set to zero and the compliance matrix were used to find the macro strains matching this stress state. A strain value of 0.16 are used for the material tests.

In the plotted results, the 1 axis is defined as the fiber direction while the 2, 3 axes are the transverse directions.

6.1.2. **Results**

On the following pages, the stress strain curves for the different single stress component load cases for three different material model sets are tested. The average stresses are plotted against the load case stress components' and corresponding strain throughout the simulations.

Test: Tension and compression in fiber direction

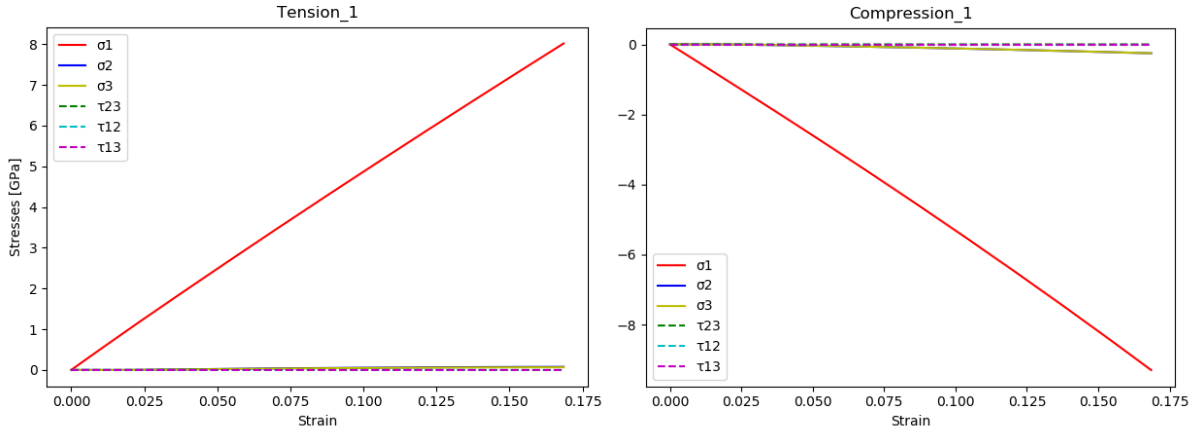

Figure 6.2: Stress strain curves for loading in fiber direction with plasticity only

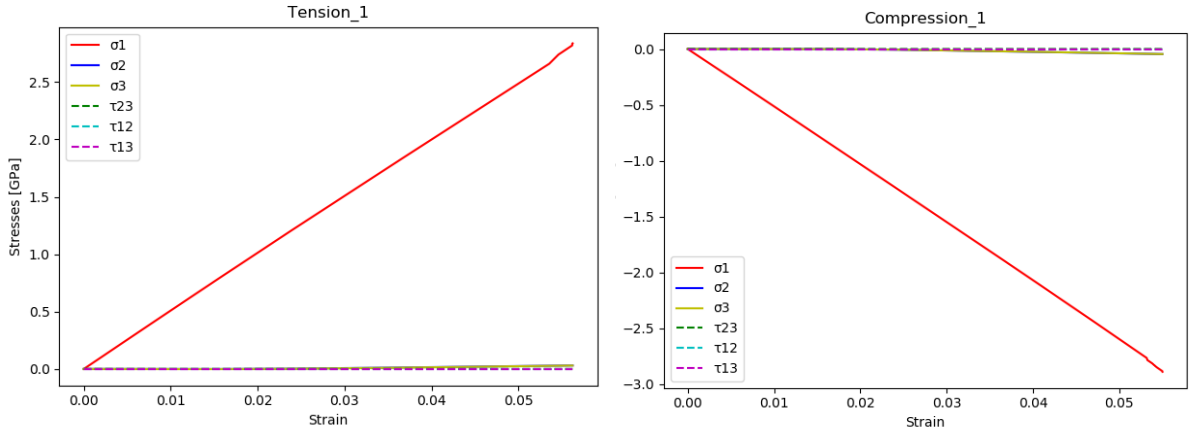

Figure 6.3: Stress strain curves for loading in fiber direction with plasticity and matrix damage

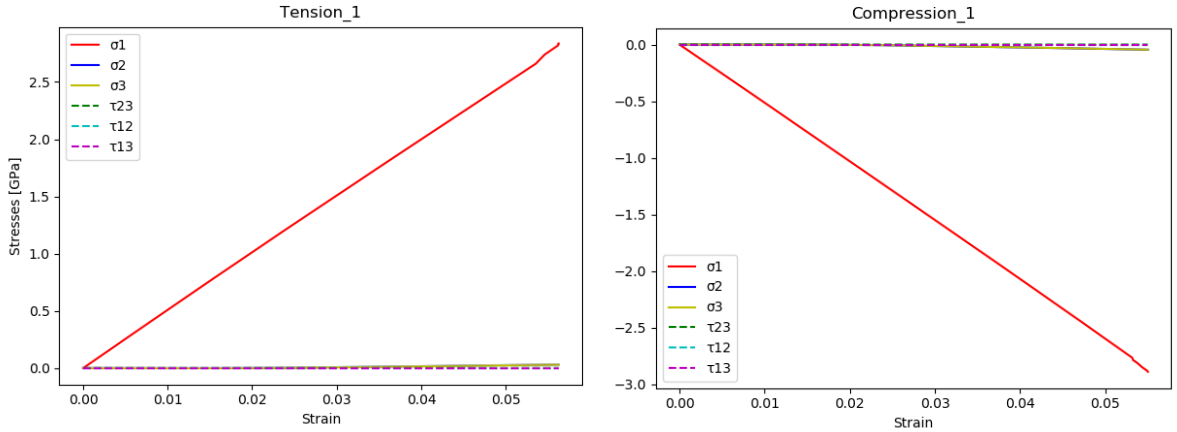

Figure 6.4: Stress strain curves for loading in fiber direction with plasticity, matrix damage and interface degradation

Test: Tension and compression transverse directions

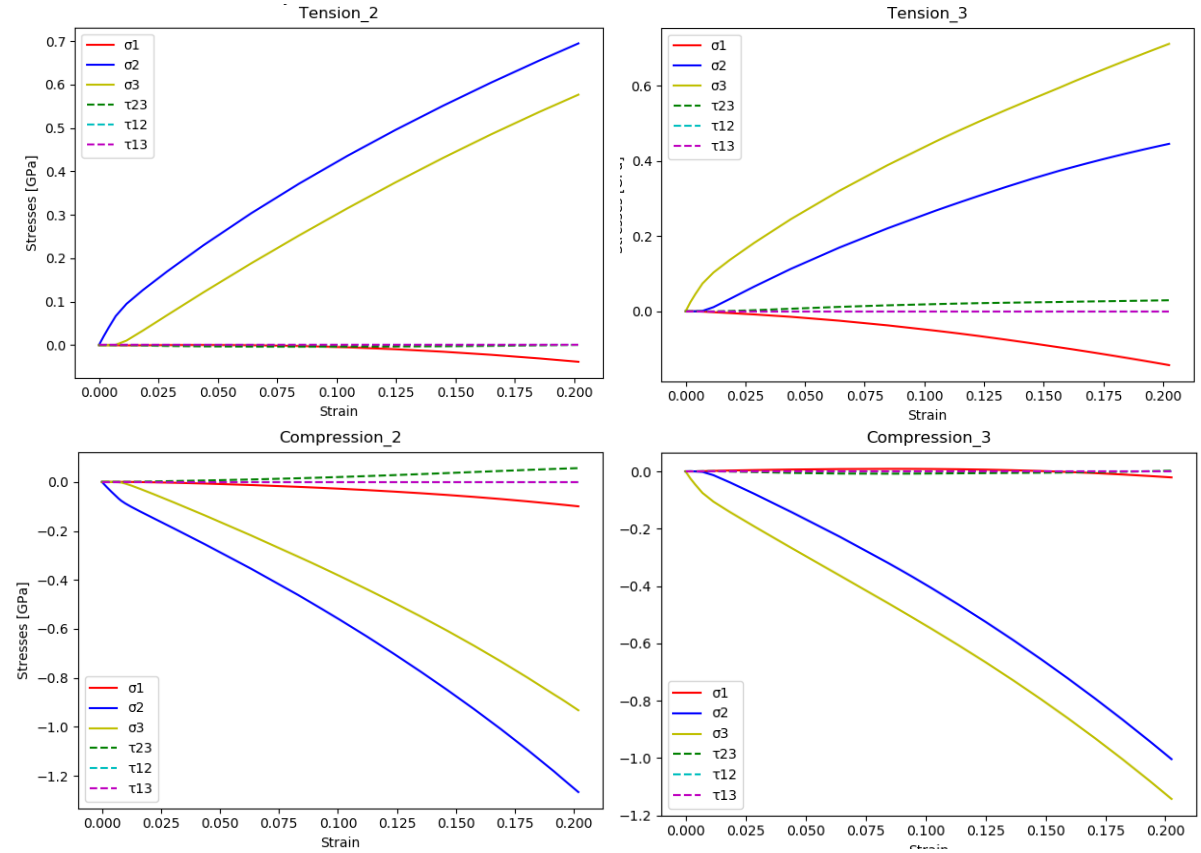

Figure 6.5: Stress strain curves for transverse loading with plasticity only

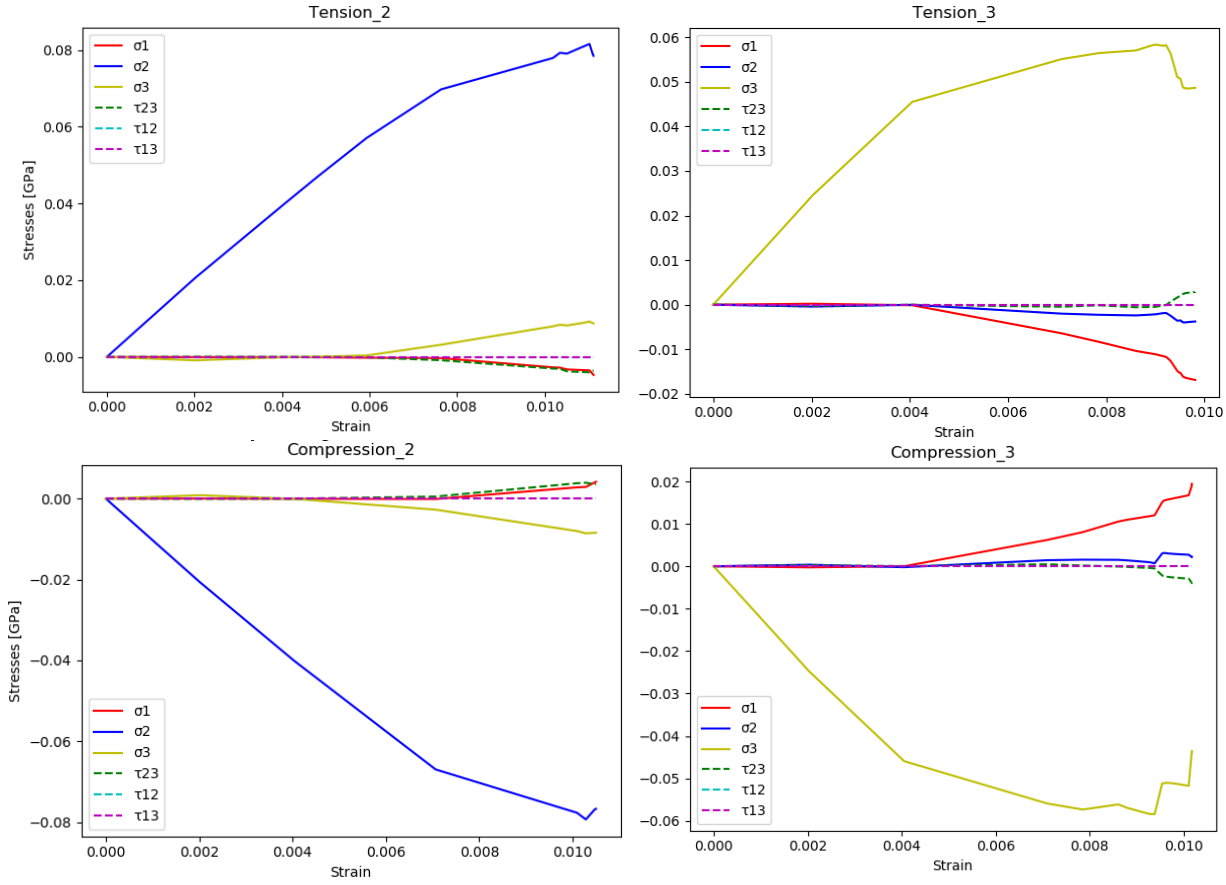

Figure 6.6: Stress strain curves for transverse loading with plasticity and matrix damage

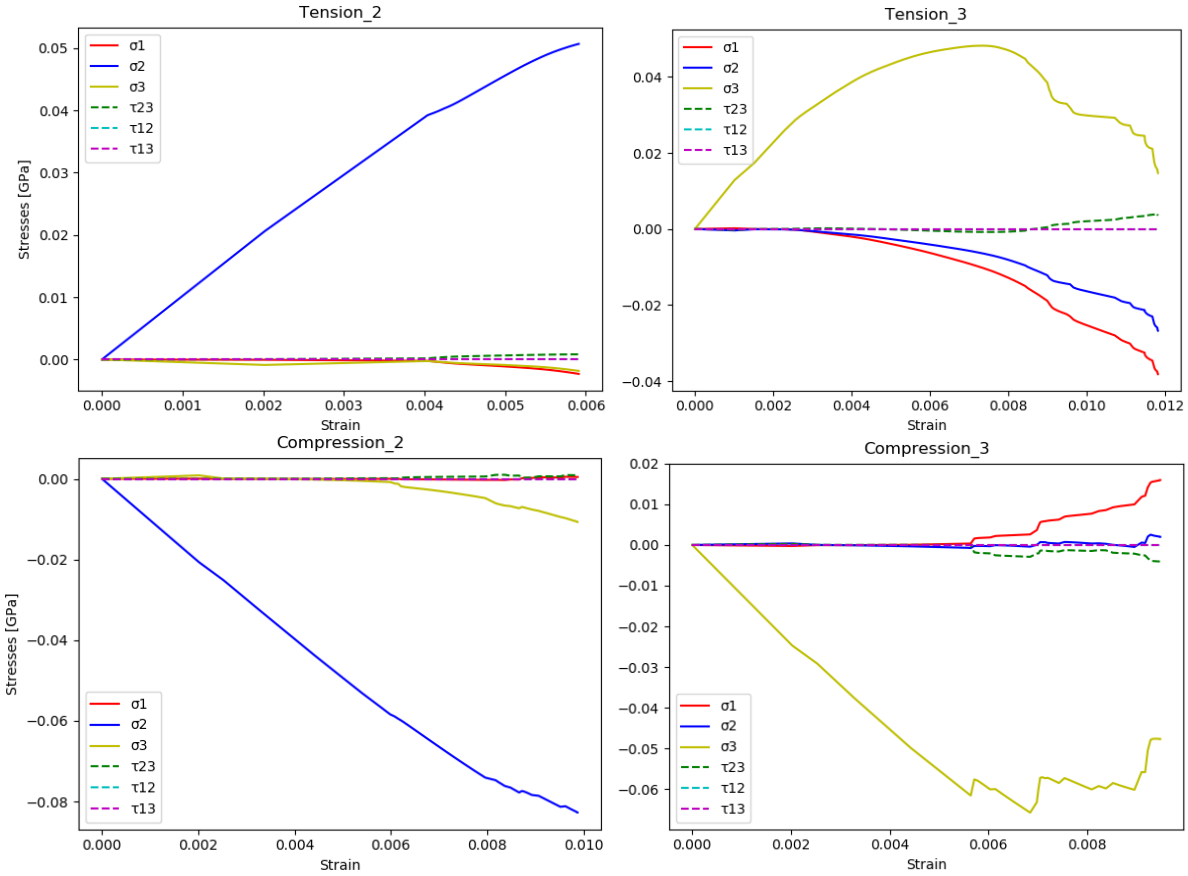

Figure 6.7: Stress strain curves for transverse loading with plasticity, matrix damage and interface degradation

Test: Shear in 2 - 3 direction

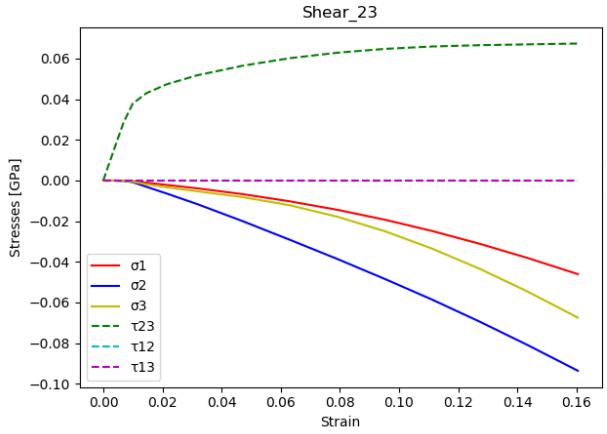

Figure 6.8: Stress strain curves for transverse shear loading with plasticity only

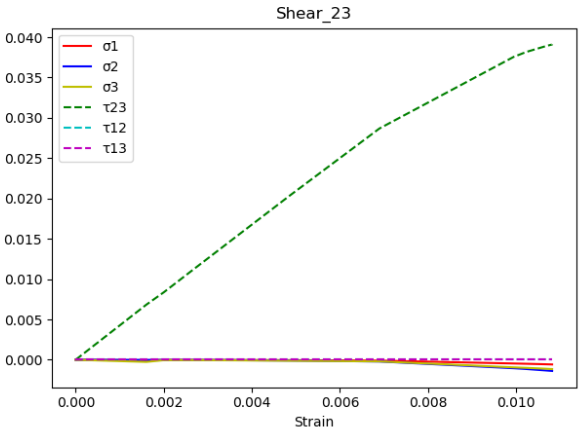

Figure 6.9: Stress strain curves for transverse shear loading with plasticity and matrix damage

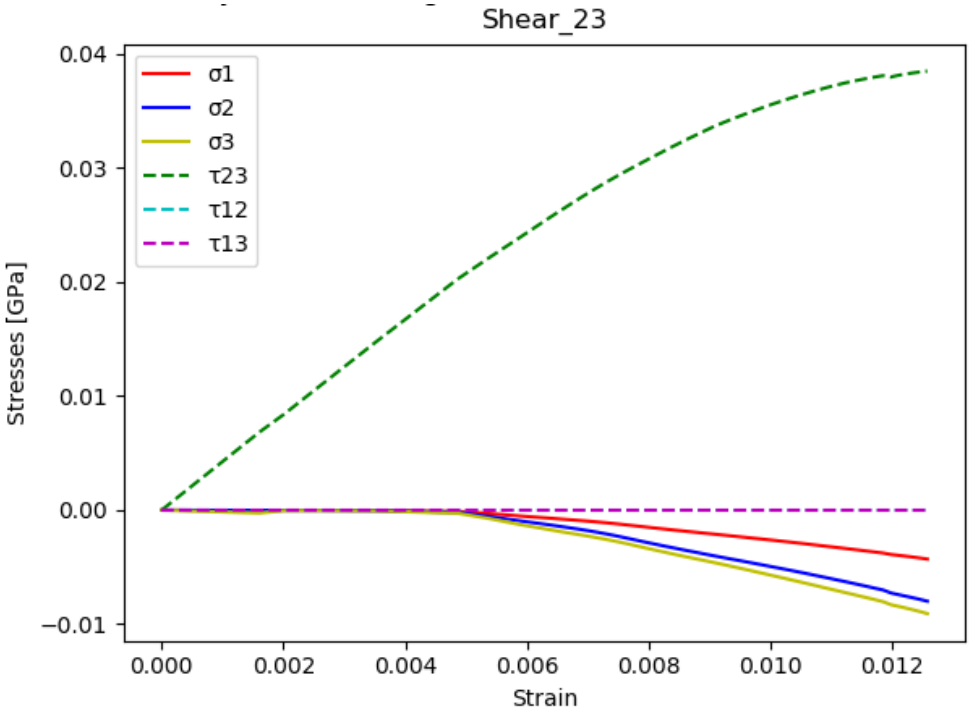

Figure 6.10: Stress strain curves for transverse shear loading with plasticity, matrix damage and interface degradation

Test: Shear in 1-2 and in 1- 3 direction

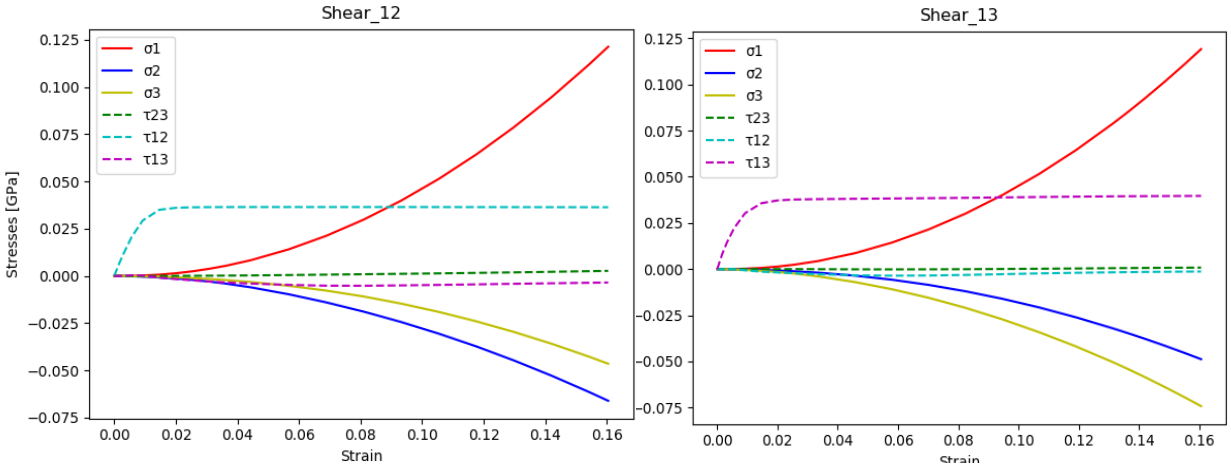

Figure 6.11: Stress strain curves for fiber parallel shear loading with plasticity only

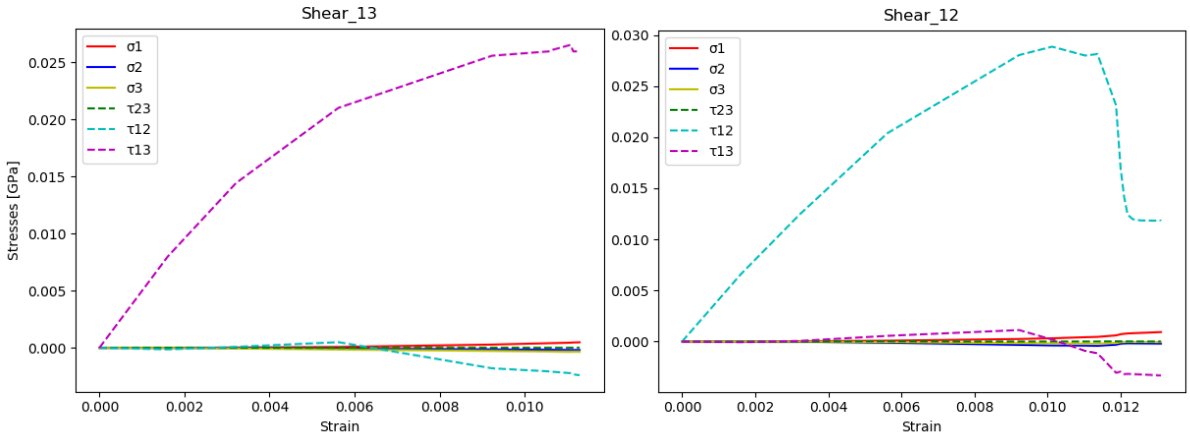

Figure 6.12: Stress strain curves for fiber parallel shear loading with plasticity and matrix damage

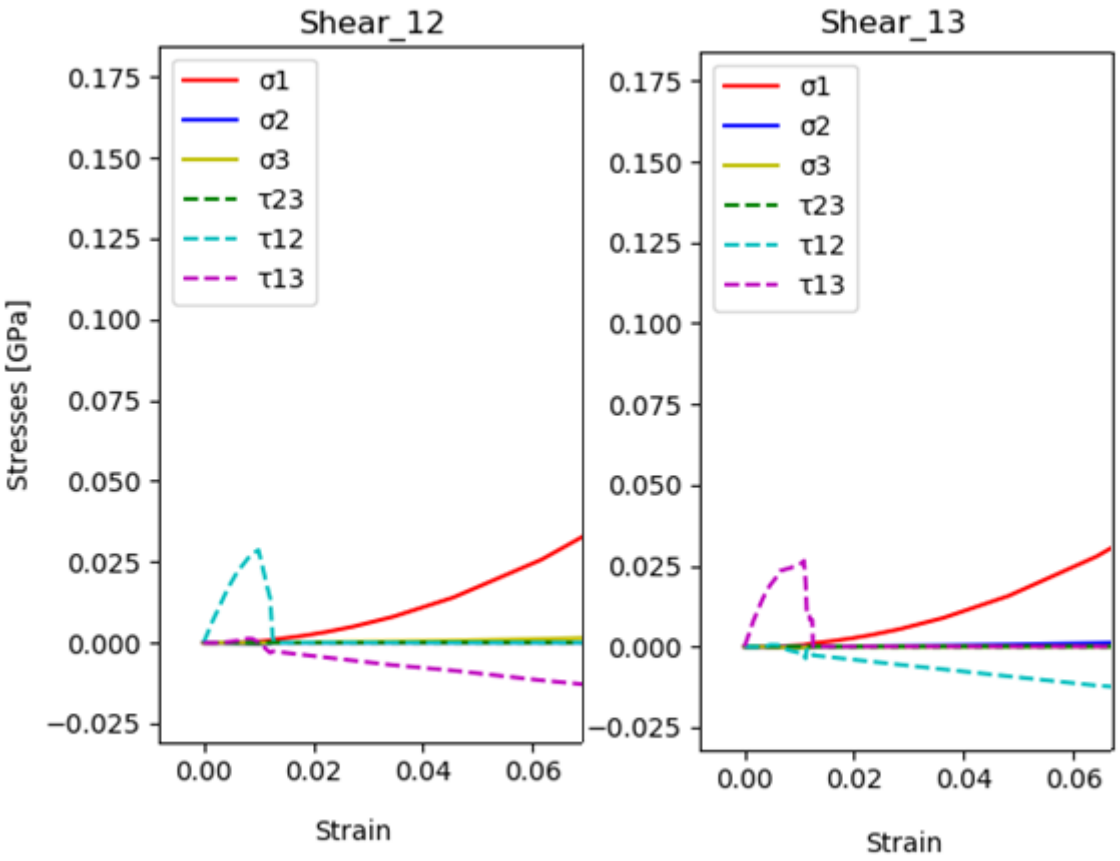

Figure 6.13: Stress strain curves for fiber parallel shear loading with plasticity, matrix damage and interface degradation

6.2. Biaxial stress tests

In this section multiaxial tests for different types of transverse stresses are explored. Equal tension2-tension3, tension2-compression3, compression2-tension3 and compression2-compression3 stresses were imposed on the ten-fiber RVE model with plasticity, matrix damage and interface delamination. A strain value of 0.08 is used to find the stresses in the biaxial tests.

Test: Biaxial loads in 2-3 transverse directions

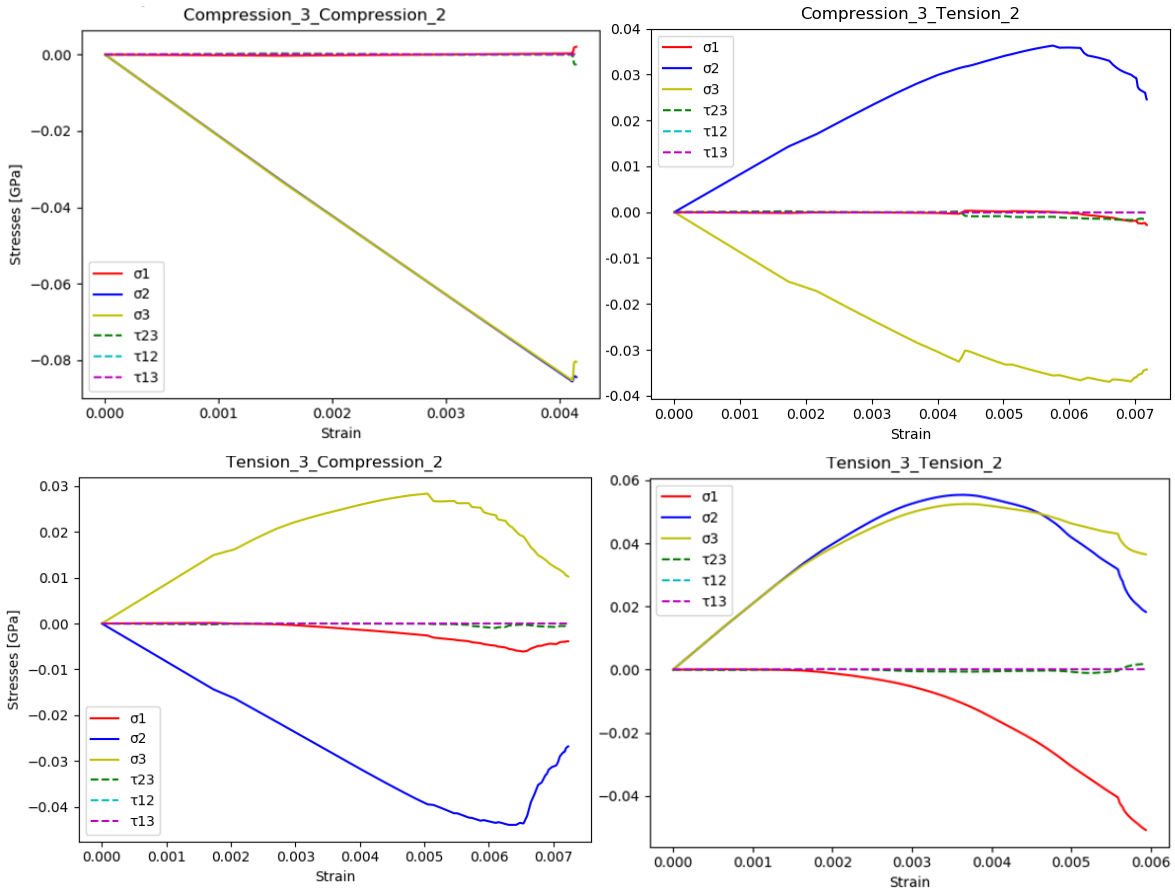

Figure 6.14: Stress strain curves for biaxial transverse loading with plasticity, matrix damage and interface degradation.

Creating Envelopes

In Figure 6.15, the results of the 2-3 biaxial and the 2 and 3 uniaxial tests are plotted to create a rough failure envelope. The inner envelope shows the interface damage initiation in the tension-comporession cases. The other envelope shows the first element damage occurance. A finer resolution of loadcases is requiered for a more accurate envelope shape.

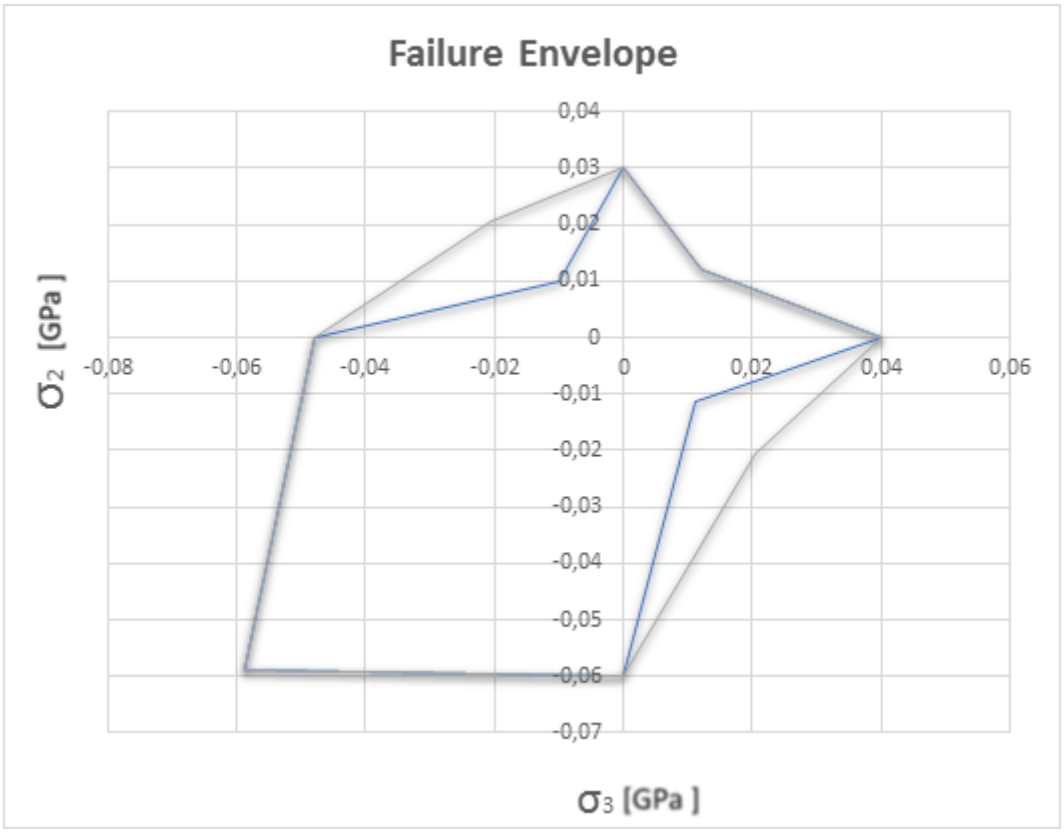

Figure 6.15: An 8-point failure envelope showing initial damage for plasticity, matrix damage and interface degradation models

6.3. Approach to backward iteration

While the material models and stress state affect the stress strain curves, several of the simulations average stresses deviate from the initial load case throughout the simulations. These problems are almost not present in the damage and delamination cases presented, due to the small deformation before failure. While the tension 2-tension 3 load case seem to include a deviation in the average stresses, closer investigations showed that the inter-fiber matrix element failed before the stresses diverge.

Therefore, this method is investigated with plasticity models only as other possible constituent material models and damage models might allow for greater deformations than the damage models applied in this thesis.

When examining Figure 6.1 and Figure 6.16, the sharp edges on the first figure is apparent compared to the second figure. This is due to the stress divergence. When the stress is adjusted, the sharp edges soften. In Figure 6.1 is a tension manifesting in the other transverse direction as shown in graph Figure 6.5.

The backward iterative method used to maintain initial load case is described in 3.7, Strength prediction. To identify when a stress component is marked as diverging, an absolute or a relative limit can be applied. A relative approach with a limit of 5% of the loaded stresses is used to identify when a stress is diverging. The high treshold for stress divergence is used, as an optimal solution is not the goal of this investigation. Any functional method is accepted.

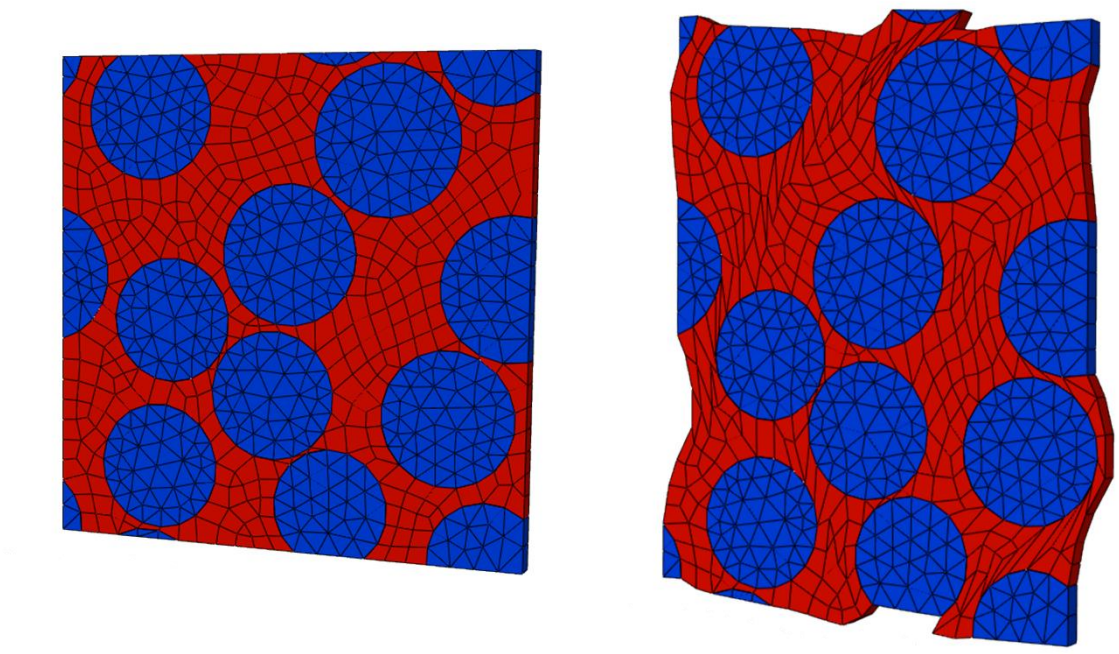

Figure 6.16: A transverse macrostrain with readjustment, intended to stretch the plastic RVE by ~10%

Test: Backward iteration to adjust load case for tension in transverse-2 direction

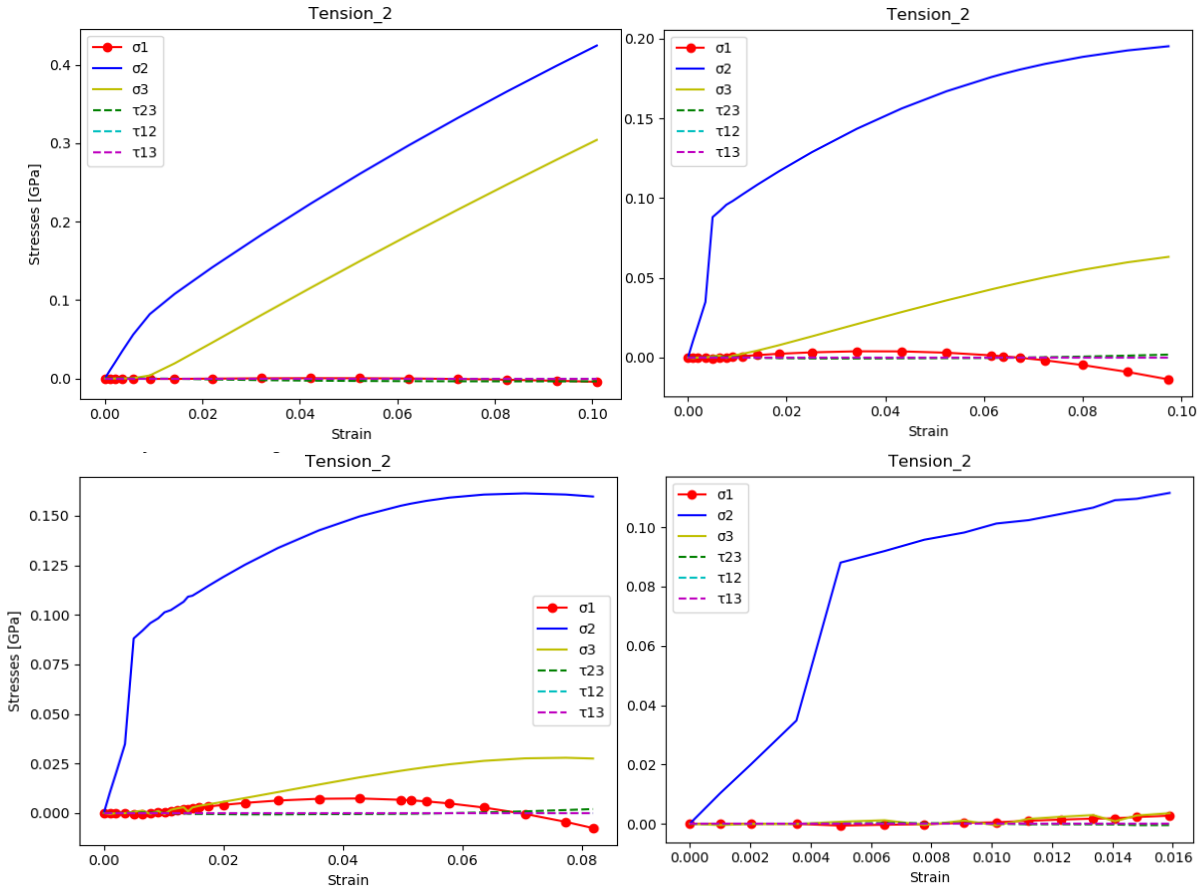

Figure 6.17: Stress strain curves showing the readjustment of the macro strains for transverse-2 tension with plasticity

Test: Backward iteration to adjust load case for shear in 1-2 direction

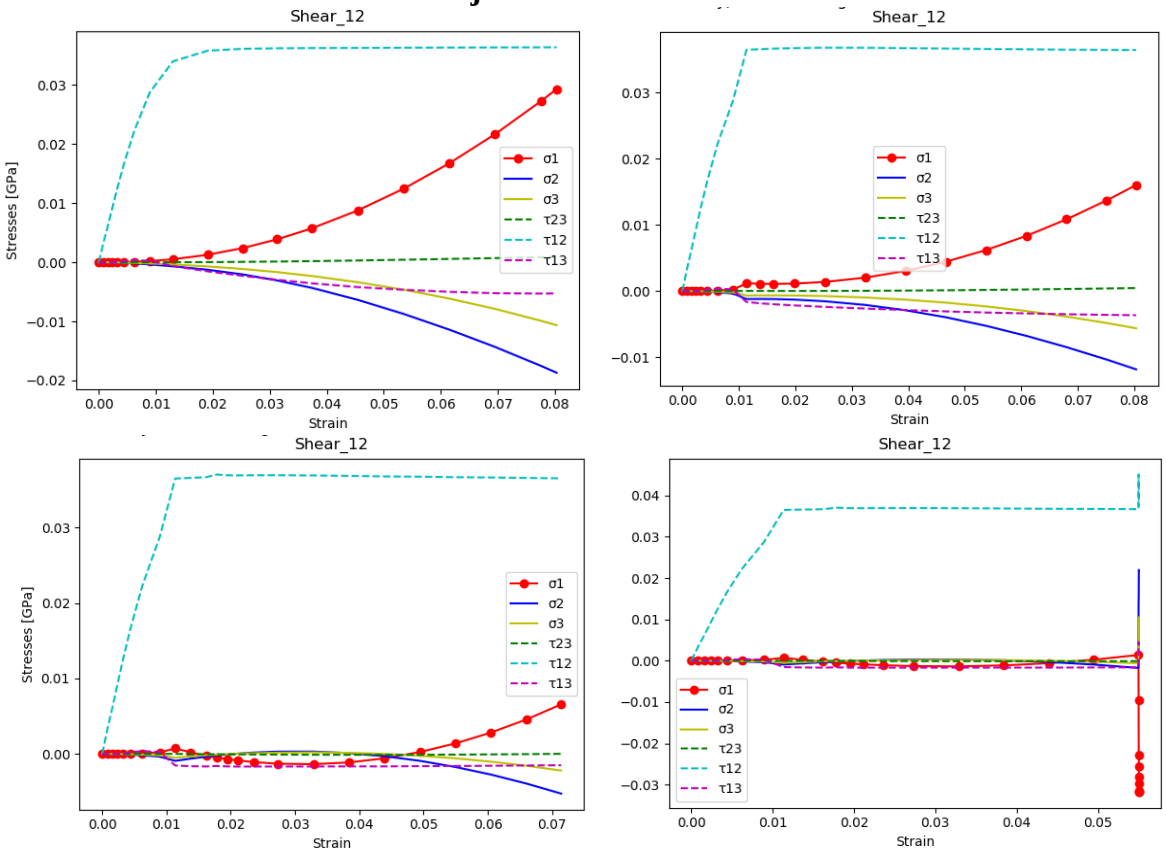

Figure 6.18: Stress strain curves showing the readjustment of the macro strains for 1-2 shear loading with plasticity

Test: Backward iteration for tension in transverse-2 and shear in 1-2 direction

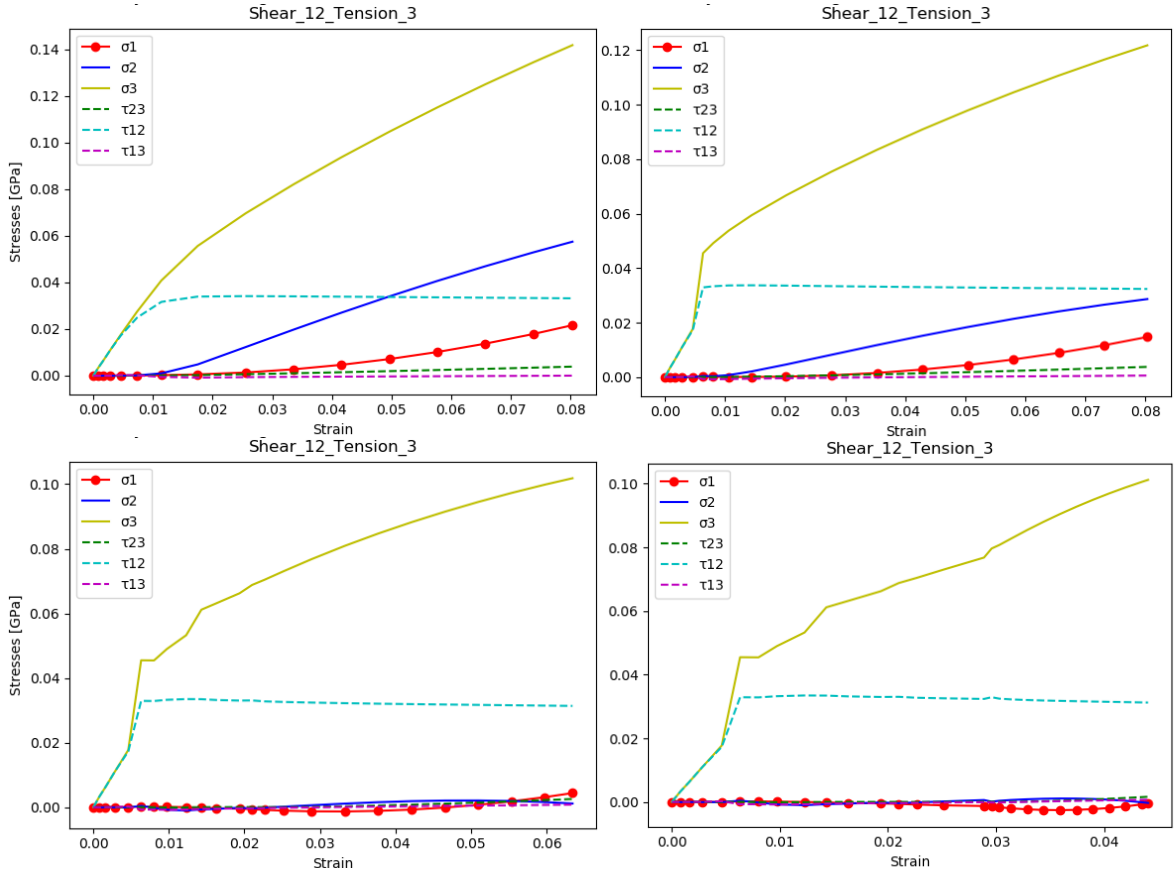

Figure 6.19: Stress strain curves showing the readjustment of the macro strains for transverse-2 tension and shear in 1-2 direction with plasticity

Test: Backward iteration of shear in 1-3 and shear in 1-2 direction

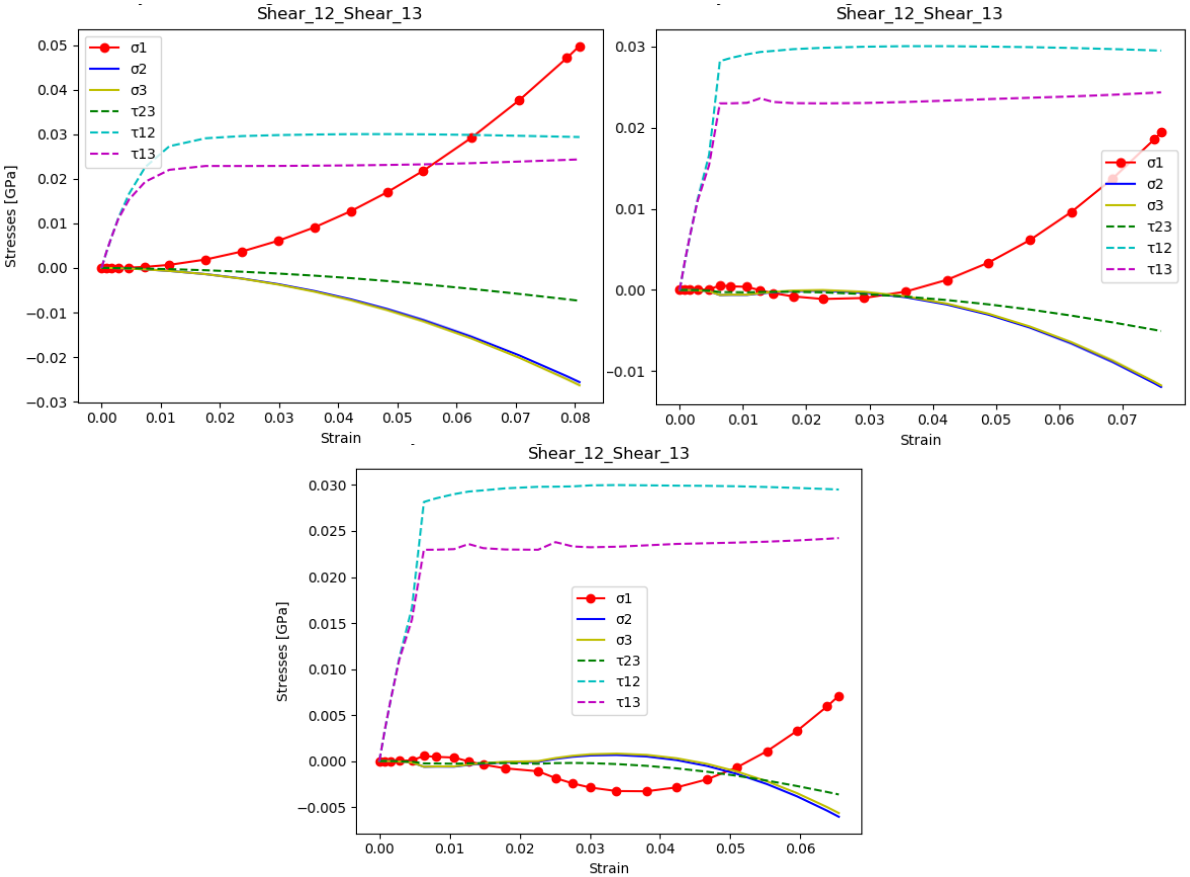

Figure 6.20: Stress strain curves showing the readjustment of the macro strains for 1-2 and 1-3 shear loading with plasticity

7. Discussion:

In this chapter the modelling, approach and results are discussed with respect to the feasibility of the applied method. After the RVE modelling is addressed, the results from chapter 4, 5 and 6 are discussed before the entirety of the tool is assessed. Afterwards, ideas for further work will be discussed.

RVE model generation

A few of the generated RVE models caused errors in the simulations. From investigating the error messages, it seems that the fiber placement algorithm allowed for some fibers to be placed, so a minuscule bit of the fiber appeared in the opposite corner of the RVE. As these corner elements were much smaller than any modelling parameters, the script malfunctioned in applying the constraint equations. When this error occurred, a new random key was assigned and a new RVE model was created. While this workaround was used, the errors show that not all fiber populations generated by the developed fiber placement algorithm are modellable by the script.

Another aspect in the modelling is the deviation in modelled fiber volume fraction in fiber populations, due to fiber variation. Currently, this parameter is free to deviate with each random key. This might cause greater deviations when performing a statistical amount of simulations, so the fiber volume fraction in the RVE models should be better constrained to obtain consistent results.

Estimation of elastic properties

The estimated elastic properties for the glass fiber correlate reasonably well with common micromechanical approximations (Hull, 1981). The modelling of an interface was shown to have little effect on the estimations, unless the interface was modelled as a weaker material. In these cases, the elastic properties in the transverse directions were affected.

The parameter investigation illustrates how changes in the different parameters can provide information about the deterministic effect of these design parameters. As stiffness tests are performed with linear behaviour, these simulations can be performed very quickly. Due to this, extensive tests for investigations of these parameters can be investigated quickly.

Linear biaxial stress cases

While these simulations were used to investigate load cases, the modelling of linear behaviour is quite limiting with respect to the investigation of physical phenomena. The envelopes produced might still be used to estimate initial load capabilities before damage initiation. Both the produced max shear stress and max principal strain envelopes indicate higher loading capabilities in the compression-compression load cases relative to the other load cases. This is a feature shared with common composite failure criteria like Hashin (Hashin, 1980) and Puck (Puck & Schürmann, 2004).

Nonlinear behaviour

While the plasticity tests in 6.1 provide little realistic insight, results from the simulations with damage models were more promising. The transverse compression cases for the damage models supports findings of González and Llorca (2007) and the transverse tension case supports the findings of Pulungan et al. (2017). In both cases, the general shape of the stress strain curves and the relative estimated values correlate reasonably well with the produced results.

The 1-2 shear strength was compared to the results from Naya et al. (2017). In this case, a similar stress strain curve was found, but the shear strength was found to be distinctly lower than the estimations from Naya et al. (2017). A reason for this might be that the simulations by Naya et al. (2017) were performed on models where the interface is modelled as a transverse isotropic material with shear stiffness constants slightly higher, and the normal stiffness constant slightly lower than the matrix's Youngs modulus. The interface material in the RVE models produced in this thesis are modelled as an isotropic material with the same properties as the matrix. This difference in the interface's elastic properties might explain the differences in estimated strength values.

The strength tests in this thesis were performed on a single RVE with slightly lower stiffness in one of the transverse directions as shown in equation (9). A similar difference was found in the transverse tension strengths in Figure 6.6 and Figure 6.7. The difference in elastic properties in the transverse directions, with a similar strengths difference in the same corresponding directions, further indicates a relationship between elastic properties in a direction and the strength in the same direction. As both the shear strength and the transverse tension strength, indicates a relationship between stiffness and strength, a relationship is assumed. This should be researched further and tested before any conclusions can be made.

Failure envelopes

The produced failure envelope presented in Figure 6.15 was based on stresses at initial failure in the elements, caused by the applied damage models. The produced envelope shares features with failure criteria like Hashin (Hashin, 1980) and Puck (Puck & Schürmann, 2004). Still, there is a need for a finer load case resolution to determine the shape of the failure envelope.

The produced envelope was based on strength test of a single ten-fiber RVE. To get an envelope which may be used to predict failure, the envelopes should be based on results from several RVE models to establish an average with a statistical deviation. The tests should also be performed on different sized RVEs to determine the effect of the RVE size.

The stresses in the produced envelope are based on stress at damage initiation. While these values were chosen for this case, several other values, like max stress and failure strain, can be extracted and used to create several different models as done for different stress variants in chapter 5.

Backward iterative process.

As shown in the figures in 6.3 the developed backward iterative method manages to influence the stresses manifesting in the RVE. While this method was sufficient to adjust the stress case back to the initial load case after the initial stress deviation, the method stagnates before massive deformation manifests. The stagnation of the process is assumed to be due to the stiffness matrix changes throughout the deformation. At one point the initial stiffness matrix is no longer a valid reference between the average stresses and the macro strains.

While this problem might be solved, the sharp edges on the figures in 6.3 are assumed to be caused by sudden changes in macro strain propagation. An approach with user subroutines in Abaqus is therefore recommended to achieve more stable load case simulations.

Accurate estimations of composite properties

As the aim of this thesis has been to investigate the modelling method, the material models and produced results are not intended to accurately portray and calculate a specific composite material. While epoxy and glass fiber material parameters are used in the investigations, accurate estimations of real composites will require specific constituent properties. In addition, the results should be confirmed with experimental results.

The simple material models used in this thesis are intended to demonstrate the effect of using different material models, and are not intended to find high fidelity estimations of composite properties. Even though element convergence tests are usually applied to increase fidelity, these are not performed in this thesis because they are outside the scope of this thesis.

Multiscale modelling of fiber composites

As demonstrated in this thesis, developing and implementing a modelling approach based on first order homogenization to perform stiffness and strength estimations in an FEA environment, is feasible. The script developed in this project can now model RVEs from given design parameters and perform stiffness and strength estimations which correlate reasonably well with similar published work. To perform high-fidelity estimations of composites with the developed tool, the results need to be confirmed with experimental results before they can be deemed accurate.

The script is now functional, but seeing that the complexity of the script increases with added content, the code should be refactored to ensure repeatability and to make further development easier and more efficient.

7.1. Ideas for further work

Thermal expansion

To investigate residual stresses developed in the curing process, the specific volume change in the RVEs constituents can be modelled (González & Llorca, 2007). To model this, mechanical thermal expansion can be implemented to the developed tool. This also allows for investigation of expansions due to thermal effect or saturations.

Improved stress tests

To better maintain load cases, user subroutines in Abaqus and Fortran should be studied. This might lead to more stable nonlinear load case simulations which might be necessary for other material models which might improve the estimations.

Interface modelling

While cohesive elements were used to model the interface in this thesis, this does not exclude the possibility of adding an option of switching between cohesive surfaces and cohesive elements in the tool. Both options are possible to use when modelling delamination, and the investigation of the different results might be interesting.

Material models

The script is organized to facilitate for implementation of new material models. This option allows for easy toggling between different material models and the possibility of cycling through several material models when performing simulations. This would allow for failure envelopes based on several possible material models. The concrete plasticity damage model used by Naya et al. (2017) has been imported to the script. By investigating other publications and getting material parameters from experiments, a library of different material models can be created to test the effects of these different models.

Inter-fiber area

A finer mesh resolution will also help in the investigation of minimum inter-fiber distance. Currently, the mesh resolution is so large that only a single element is placed between the interfaces of two closely packed fibers. With smaller mesh sizes this area can be investigated with a greater resolution which might provide insight to the effects in this area.

8. Conclusion:

A script which applies a multiscale modelling method based on a first order homogenization approach has successfully been developed and implemented in an FEA environment to model the microscale of composites and perform simulations to estimate stiffness and strength. The script is able to generate RVE models from a set of controllable design parameters and given material models to perform stiffness and strength estimations. To demonstrate the developed tool, an epoxy and glass fiber composite was modelled from simple material- and damage models.

In a brief investigation of elastic properties, the converged average from several different fiber distributions was found to converge toward similar values. It was also shown that the scatter in these results decreases as the RVE size increases, which provides a convergence from fewer samples. The strength estimates were found to correlate with findings from similar published work.

Altogether, this indicates that a script based on this method could provide practical insight to composite performance. As the project was defined as a feasibility study, the achievements from the developed tool have not been confirmed with experimental data. Before such a tool is applied in product development cases with composites, the results procured through this method should be confirmed with experimental data.

9. References

Dassult_Sysytems_Simula. (2014). Abaqus FEA documentation. *6.14-4*.

Geers, M. G. D., Kouznetsova, V. G., & Brekelmans, W. A. M. (2010). Multi-scale computational homogenization: Trends and challenges. *Journal of Computational and Applied Mathematics, 234*(7), 2175-2182. doi:https://doi.org/10.1016/j.cam.2009.08.077

González, C., & Llorca, J. (2007). Mechanical behavior of unidirectional fiber-reinforced polymers under transverse compression: Microscopic mechanisms and modeling. *Composites Science and Technology, 67*(13), 2795-2806. doi:https://doi.org/10.1016/j.compscitech.2007.02.001

Hashin, Z. (1980). Failure Criteria for Unidirectional Fiber Composites. *Journal of Applied Mechanics, 47*(2), 329-334. doi:10.1115/1.3153664

Hull, D. (1981). *An introduction to composite materials*. Cambridge University Press.

Llorca, J., González, C., Molina-Aldareguía, J. M., Segurado, J., Seltzer, R., Sket, F., . . . Canal, L. P. (2011). Multiscale Modeling of Composite Materials: a Roadmap Towards Virtual Testing. *Advanced Materials, 23*(44), 5130-5147. doi:10.1002/adma.201101683

Naya, F., González, C., Lopes, C. S., Van der Veen, S., & Pons, F. (2017). Computational micromechanics of the transverse and shear behavior of unidirectional fiber reinforced polymers including environmental effects. *Composites Part A: Applied Science and Manufacturing, 92*, 146-157. doi:https://doi.org/10.1016/j.compositesa.2016.06.018

Petersen, H. N. (2017). *Investigation of sizing - from glass fibre surface to composite interface.*

Puck, A., & Schürmann, H. (2004). Chapter 5.6 - Failure analysis of FRP laminates by means of physically based phenomenological models A2 - Hinton, M.J. In A. S. Kaddour & P. D. Soden (Eds.), *Failure Criteria in Fibre-Reinforced-Polymer Composites* (pp. 832-876). Oxford: Elsevier.

Pulungan, D., Lubineau, G., Yudhanto, A., Yaldiz, R., & Schijve, W. (2017). Identifying design parameters controlling damage behaviors of continuous fiber-reinforced thermoplastic composites using micromechanics as a virtual testing tool. *International Journal of Solids and Structures, 117*, 177-190. doi:https://doi.org/10.1016/j.ijsolstr.2017.03.026

Romanov, V., Lomov, S. V., Swolfs, Y., Orlova, S., Gorbatikh, L., & Verpoest, I. (2013). Statistical analysis of real and simulated fibre arrangements in unidirectional composites. *Composites Science and Technology, 87*, 126-134. doi:https://doi.org/10.1016/j.compscitech.2013.07.030

Swaminathan, S., Ghosh, S., & Pagano, N. J. (2005). Statistically Equivalent Representative Volume Elements for Unidirectional Composite Microstructures: Part I - Without Damage. *Journal of Composite Materials, 40*(7), 583-604. doi:10.1177/0021998305055273

Vedvik, N. P. (2017). TMM4175 Composite design.

Wang, K., & Sun, W. (2016). *A semi-implicit micropolar discrete-to-continuum method for granular materials*.